NASA/CR—2008-215235

Intelligent Engine Systems

Acoustics

John Wojno, Steve Martens, and Benjamin Simpson
General Electric Aircraft Engines, Cincinnati, Ohio

June 2008

NASA STI Program . . . in Profile

Since its founding, NASA has been dedicated to the advancement of aeronautics and space science. The NASA Scientific and Technical Information (STI) program plays a key part in helping NASA maintain this important role.

The NASA STI Program operates under the auspices of the Agency Chief Information Officer. It collects, organizes, provides for archiving, and disseminates NASA's STI. The NASA STI program provides access to the NASA Aeronautics and Space Database and its public interface, the NASA Technical Reports Server, thus providing one of the largest collections of aeronautical and space science STI in the world. Results are published in both non-NASA channels and by NASA in the NASA STI Report Series, which includes the following report types:

- TECHNICAL PUBLICATION. Reports of completed research or a major significant phase of research that present the results of NASA programs and include extensive data or theoretical analysis. Includes compilations of significant scientific and technical data and information deemed to be of continuing reference value. NASA counterpart of peer-reviewed formal professional papers but has less stringent limitations on manuscript length and extent of graphic presentations.

- TECHNICAL MEMORANDUM. Scientific and technical findings that are preliminary or of specialized interest, e.g., quick release reports, working papers, and bibliographies that contain minimal annotation. Does not contain extensive analysis.

- CONTRACTOR REPORT. Scientific and technical findings by NASA-sponsored contractors and grantees.

- CONFERENCE PUBLICATION. Collected papers from scientific and technical conferences, symposia, seminars, or other meetings sponsored or cosponsored by NASA.

- SPECIAL PUBLICATION. Scientific, technical, or historical information from NASA programs, projects, and missions, often concerned with subjects having substantial public interest.

- TECHNICAL TRANSLATION. English-language translations of foreign scientific and technical material pertinent to NASA's mission.

Specialized services also include creating custom thesauri, building customized databases, organizing and publishing research results.

For more information about the NASA STI program, see the following:

- Access the NASA STI program home page at *http://www.sti.nasa.gov*

- E-mail your question via the Internet to *help@sti.nasa.gov*

- Fax your question to the NASA STI Help Desk at 301–621–0134

- Telephone the NASA STI Help Desk at 301–621–0390

- Write to:
  NASA Center for AeroSpace Information (CASI)
  7115 Standard Drive
  Hanover, MD 21076–1320

NASA/CR—2008-215235

Intelligent Engine Systems

Acoustics

John Wojno, Steve Martens, and Benjamin Simpson
General Electric Aircraft Engines, Cincinnati, Ohio

Prepared under Contract NAS3–01135, Work element 3.3, Task order 37

National Aeronautics and
Space Administration

Glenn Research Center
Cleveland, Ohio 44135

June 2008

This work was sponsored by the Fundamental Aeronautics Program at the NASA Glenn Research Center.

Level of Review: This material has been technically reviewed by NASA technical management.

Available from

NASA Center for Aerospace Information
7115 Standard Drive
Hanover, MD 21076–1320

National Technical Information Service
5285 Port Royal Road
Springfield, VA 22161

Available electronically at http://gltrs.grc.nasa.gov

Intelligent Engine Systems
Acoustics

John Wojno, Steve Martens, and Benjamin Simpson
General Electric Aircraft Engines
Cincinnati, Ohio 45215

Objectives

The objective of this Work Element is to explore and optimize low noise fan exhaust nozzle designs for noise reduction and improved performance using variable geometry. This will include using shape memory alloy materials in the fan nozzle to optimize noise reduction during noise sensitive operations and, through variable geometry, optimize the performance impact at cruise conditions. The noise reduction concepts to be explored include advanced chevrons or other enhanced mixing concepts. The variable geometry design will feature a passive system, reacting to changing temperature conditions.

Subtask 3.3.1 UC Low-Noise Fan Nozzle Screening

Task Statement

The goal of this subtask was to support the development of next-generation low noise fan nozzles. The University of Cincinnati (UC) will provide a cost-effective means of screening a number of novel nozzle designs, to identify which have the most potential for acoustic benefit. The most promising concepts will be transitioned to GE Aviation for acoustic evaluation in Cell 41. The design space for the initial screening will necessarily be broad, examining a number of chevron and enhanced mixing configurations.

Results

The team reviewed existing model scale screening nozzle data to identify traditional fan nozzle geometries to provide acoustic benefit. Candidate chevron nozzle geometries have previously been identified that provided acoustic benefit relative to a conic exhaust nozzle, when tested in the UC jet noise facility. The parametric values that defined the corresponding chevron geometries, specifically chevron number, aspect ratio and penetration, were included in the design space for the fan chevron nozzle computational design studies performed under Subtask 3.3.2. In addition to traditional chevron nozzle designs, new devices were developed to achieve enhanced mixing, to reduce jet mixing noise.

New enhanced mixing devices were developed that are GE Proprietary. Consequently, any details of the design and testing are presented in the corresponding GE Proprietary report ONLY. To demonstrate the level of effort and the overall success of the new technology, all discussion below is limited to the overall acoustic effectiveness in general terms, with no specific description of the devices.

To simplify the development of the new enhanced mixing technology concepts, they were initially demonstrated on single flow jets. Since the UC jet acoustics facility is designed for dual-flow exhaust nozzles, the initial data were collected for single-flow application to the core exhaust nozzle, in a single flow operating condition. The resulting OASPL benefit varied from 1 to 2.5 dB, as a function of directivity. At all directivities, the new technology provided equivalent or better acoustic benefit, on an OASPL basis, than a typical chevron exhaust nozzle design.

Following successful single-flow testing, the enhanced mixing technology was tested applied to core exhaust nozzles in dual-flow operation. As expected, propagation of the core jet noise through the external shear layer at the fan-quiescent flow interface reduced the overall benefit of all low noise exhaust nozzles in dual-flow operation, relative to the single-flow performance. However, approximately 1dB of benefit was obtained from the new technology at the aft angles.

The initial tests successfully demonstrated application of the new technology to a core nozzle, which operates in the strong shear layer generated at the core and fan flow interface in a dual-flow exhaust nozzle. However, the fan shear layer can dominate jet acoustics in modern exhaust nozzle designs, particularly for high bypass ratio engine applications. Consequently, additional screening testing was performed with the enhanced mixing technology applied to a fan exhaust nozzle, with a baseline conic core nozzle, in dual-flow conditions.

Acoustic performance comparisons are shown in Figures 1-4 for the enhanced mixing technology applied to a dual flow fan nozzle, with no external flow. Figures 1 and 2 show the spectral and OASPL performance of the new enhanced mixing nozzle (12DVG) relative to a baseline conic and traditional fan chevron nozzle (16HP), for low shear cycle point representative of current commercial engine designs. The spectral data in Figure 1 demonstrate a characteristic low-frequency benefit with a corresponding high frequency lift, similar to a traditional chevron design. The low frequency benefit at this operating condition was similar to the traditional chevron nozzle, with somewhat higher high frequency penalty. Corresponding OASPL directivity data is shown in Figure 2. The OASPL data indicate that the acoustic benefit of the new technology was comparable to a traditional chevron nozzle. Similar data are presented in Figures 3 and 4 for a higher speed cycle point, representing a higher shear operating condition. These data indicate that the low frequency benefit was actually better for the new

enhanced mixing technology nozzle, relative to the traditional chevron design, resulting in somewhat improved OASPL performance at large angles to the jet axis. However, enhancement of the high frequency penalty for the new technology nozzle caused modest performance degradation, 90 degrees from the jet axis.

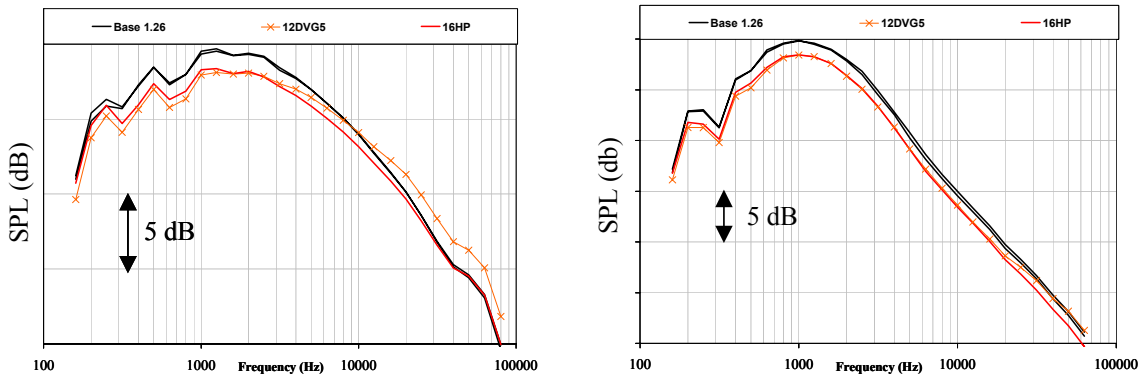

a. 90° Spectra *b. 150° Spectra*

Figure 1. Spectral Comparisons of an Enhanced Mixing Technology Fan Nozzle, Relative to Baseline Conic and Traditional Chevron Designs
Test Case #1 - Low Shear (no external flow)

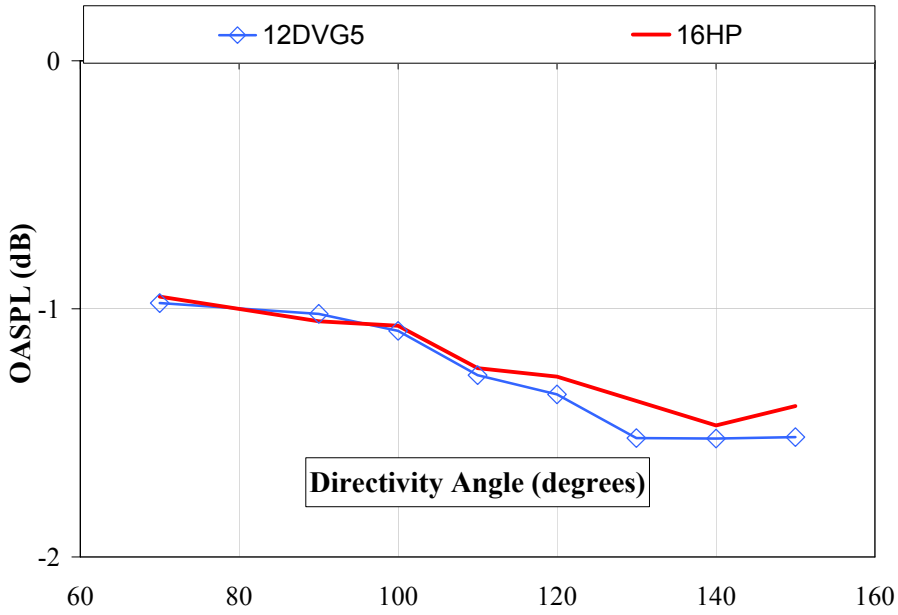

Figure 2. OASPL Benefit of an Enhanced Mixing Technology Fan Nozzle –
Test Case #1 - Low Shear (no external flow)

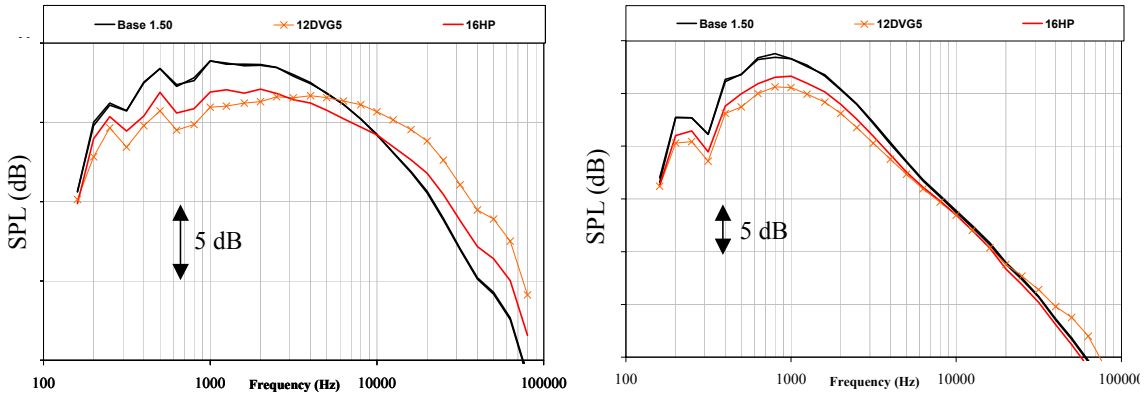

a. 90° Spectra *b. 150° Spectra*

Figure 3. Spectral Comparisons of an Enhanced Mixing Technology Fan Nozzle, Relative to Baseline Conic and Traditional Chevron Designs
Test Case #2 - High Shear (no external flow)

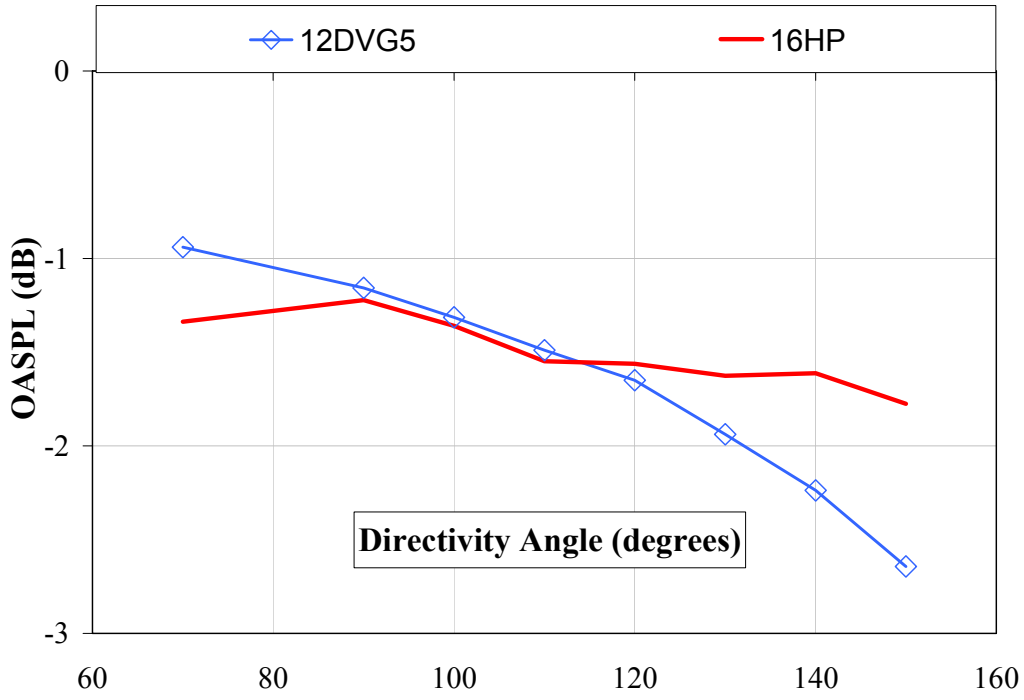

Figure 4. OASPL Benefit of an Enhanced Mixing Technology Fan Nozzle,
Test Case #2 - High Shear (no external flow)

Summary

The results of the small-scale screening testing at UC were very promising. Candidate chevron nozzle geometries were identified that demonstrated significant benefit relative to a baseline conic nozzle. In addition, new devices were developed which demonstrate acoustic benefits similar to a traditional chevron nozzle design.

However, all of the initial screening data shown above were collected in the UC Jet Noise Facility, on a generic small-scale nozzle, with no pylon, bifurcations or tertiary flow. Given the limitations of the UC facility, the TRL for the initial effort was nominally 3-4. In order to bring the new exhaust nozzle technology concept to a higher TRL, a similar geometry was selected for additional testing on more realistic scale models, in GE's jet acoustics facility, Cell 41. In addition to larger size and realistic geometric features, such as bifurcations and a pylon, testing in Cell 41 enabled assessment of the acoustic benefit in simulated flight conditions, with a more realistic fan shear layer fan established between the fan exhaust jet and a tertiary flow.

Finally, in addition to performing the initial technology screening testing at their facility, UC provided on-site test support at Cell 41 for TRL 5 model scale testing under Subtask 3.3.2. This support included acoustics data acquisition and reduction assistance, as well as providing and operating a stereo Particle Image Velocimetry (PIV) system for a limited set of cross-stream velocity measurements downstream of the core plug. The results of all of the Cell 41 testing are presented below.

Subtask 3.3.2 Next-Generation Low-Noise Fan Nozzle

Task Statement

The goal of this subtask is to investigate the effectiveness of novel fan exhaust nozzle designs in GE Aviation's Cell 41 jet acoustics facility, with external flow simulation on representative bypass ratio separate flow models. This effort will leverage nozzle concept screening evaluations being performed in Subtask 3.3.1, by UC. Initial screening data from UC will be used to identify potential candidate designs for more realistic simulation in Cell 41. The most promising concepts will be applied to complex pylon/bifurcated geometries, and evaluated with full engine cycle and external flow effects.

Results

To minimize hardware development costs, GE identified two existing model scale exhaust systems for development and testing of low-noise fan nozzle technologies. An existing medium bypass ratio (BPR ~5-6) exhaust system model, representative of current small commercial engine applications, was the primary test configuration. Five new fan chevron nozzles were fabricated for acoustic testing on this model, as outlined below. In addition, the new enhanced mixing technology exhaust nozzle concepts developed in Subtask 3.3.1 were tested, to assess the potential for acoustic benefit, relative to traditional chevron nozzle designs. Since they represented a completely new technology, these concepts were tested on both the medium BPR scale mode (BPR ~ 5-6), as well as an existing high bypass ratio (BPR~8-9) scale model exhaust system, which is more representative of large commercial engine designs.

Design Study

To commence the development of low-noise medium BPR fan nozzles, a parametric design space was defined for a CFD study of uniform fan chevron nozzle designs, as shown in Table 1. Exploring this design space, an extensive "Design of Experiment" (DOE) CFD Study was performed, using a 3D Reynold's Averaged Navier Stokes (RANS) code, PAB3D. The chevron nozzles were modeled based on a single chevron, assuming geometric symmetry. Comparisons were made to estimate the impact of each chevron design on several parameters that are expected to correlate with the strength of mixing in the shear layers, which governs the jet acoustics. The specific parameters considered were the jet total temperature, velocity, and turbulent kinetic energy (TKE). Based on the results of the CFD analyses, three new uniform fan chevron nozzles were selected for fabrication and acoustic testing on the BPR 5 model in GE Aviation's jet noise facility, Cell 41, which can be identified by bold type in Table 1.

Table 1. – Design space for Uniform Chevron DOE

CFD Case			
Relative Chevron Length	**Penetration**		
	Low	***Medium***	*High*
Short	2	3	4
Medium-Short	5	**6**	7
Medium	8	9	10
Medium-Long	**11**	**12**	13
Long	14	15	16

Notes:

1. *Case 1 was a simple conic nozzle*
2. *Cases in* **BOLD** *type were selected for fabrication & testing.*

Sample data comparisons are presented in Figures 5-6, below. These figures show the predicted cross-sectional distribution of the parameters through the jet at six axial locations: at the fan exit, and at 1, 2, 3, 4 and 5 fan nozzle geometric diameters downstream. The sample data provided below are all for Case 12, one of the designs that were selected for fabrication and testing. Consider the predicted levels of all three parameters, four diameters downstream (4D). In Figure 5, the strength of the outer shear layer for the conic nozzle is clearly strong, as evidenced by the red TKE "Hot Spot" in the fan stream. In contrast, the corresponding TKE distribution for the chevron nozzle is primarily yellow, indicating lower predicted turbulence levels in the downstream regions which have previously been shown to correlate with low frequency jet noise. This is a result of improved mixing due to the stream-wise vortical structures generated by the chevrons. The vorticity is evident by the slope in the shear layer gradient exhibited by the Total Temperature and Velocity data for the chevron at that location, which are highlighted by a dotted red line in Figures 6 and 7, respectively. Returning to Figure 5, the predicted TKE levels for the chevron nozzle two diameters downstream (2D) exhibit a red "hot spot," indicating enhanced mixing and turbulence production just aft of chevrons. This early mixing was expected to mix out the mean shear gradient that is largely responsible for the low frequency jet noise. The primary question was whether a large high frequency penalty was incurred by the mixing.

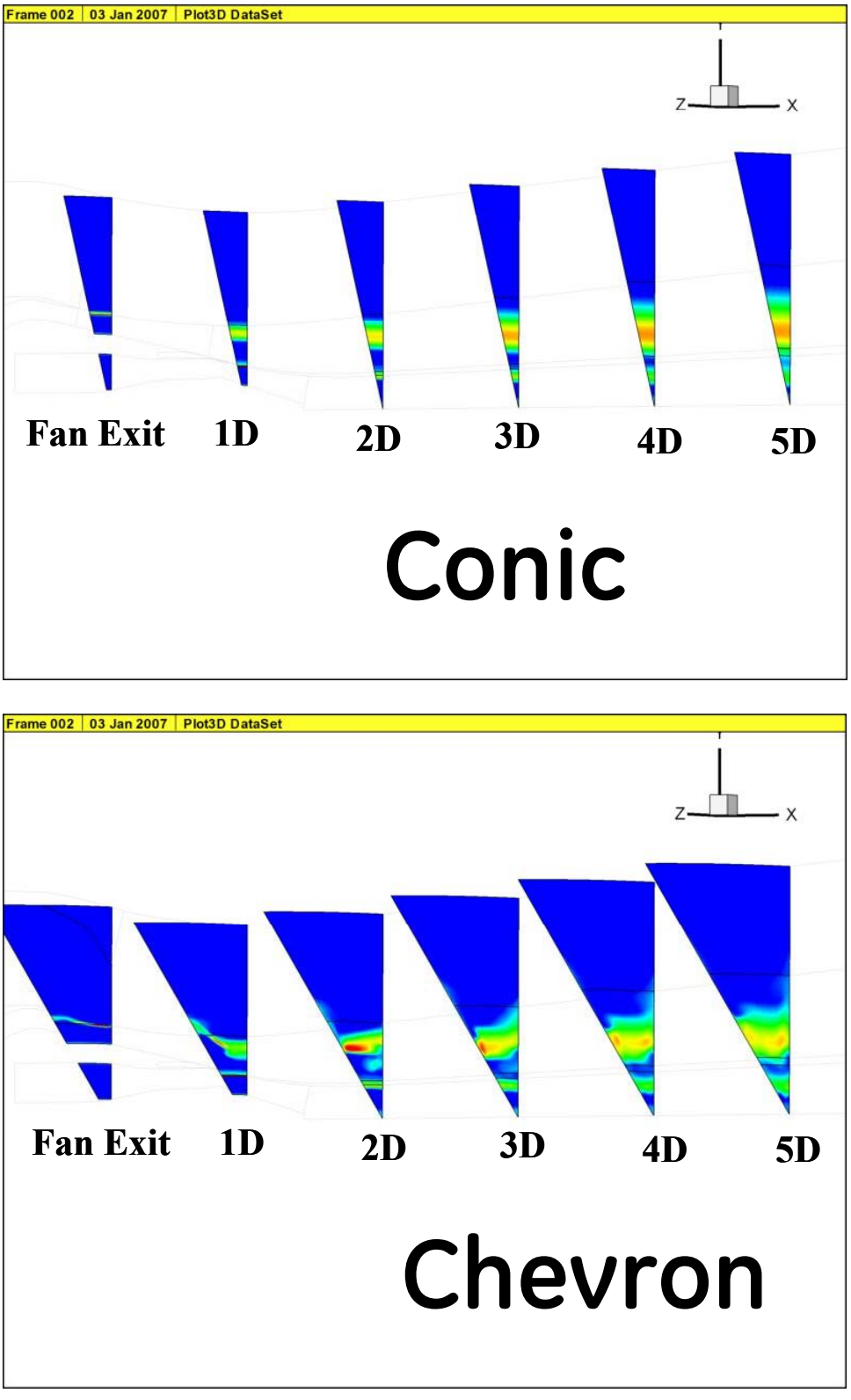

Figure 5. Jet TKE Distribution Comparison

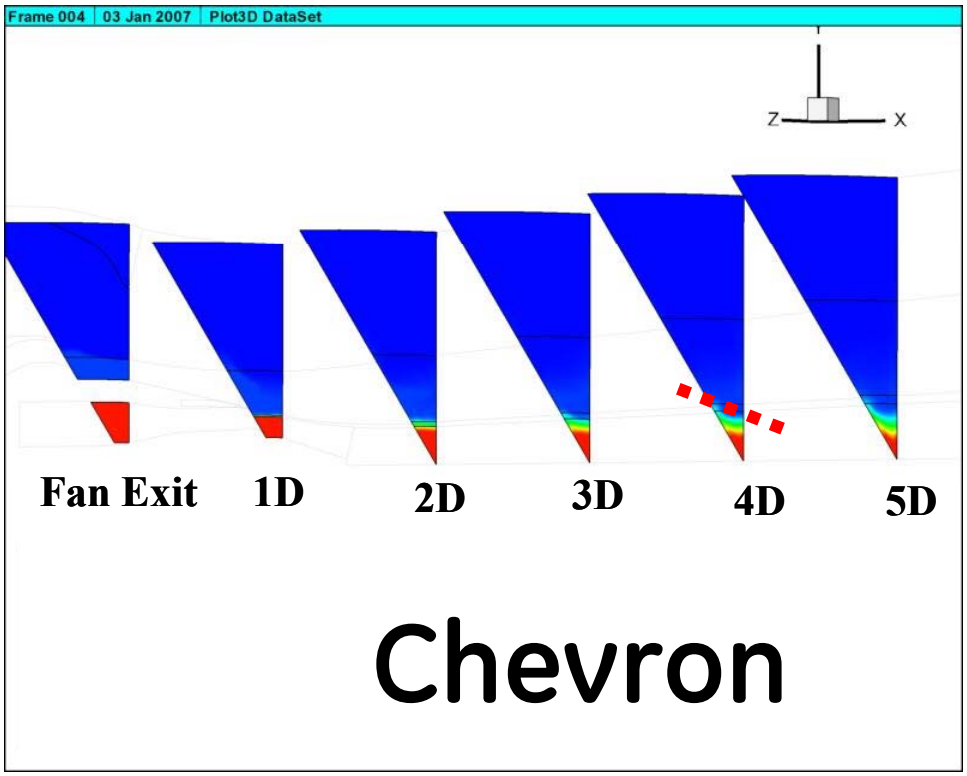

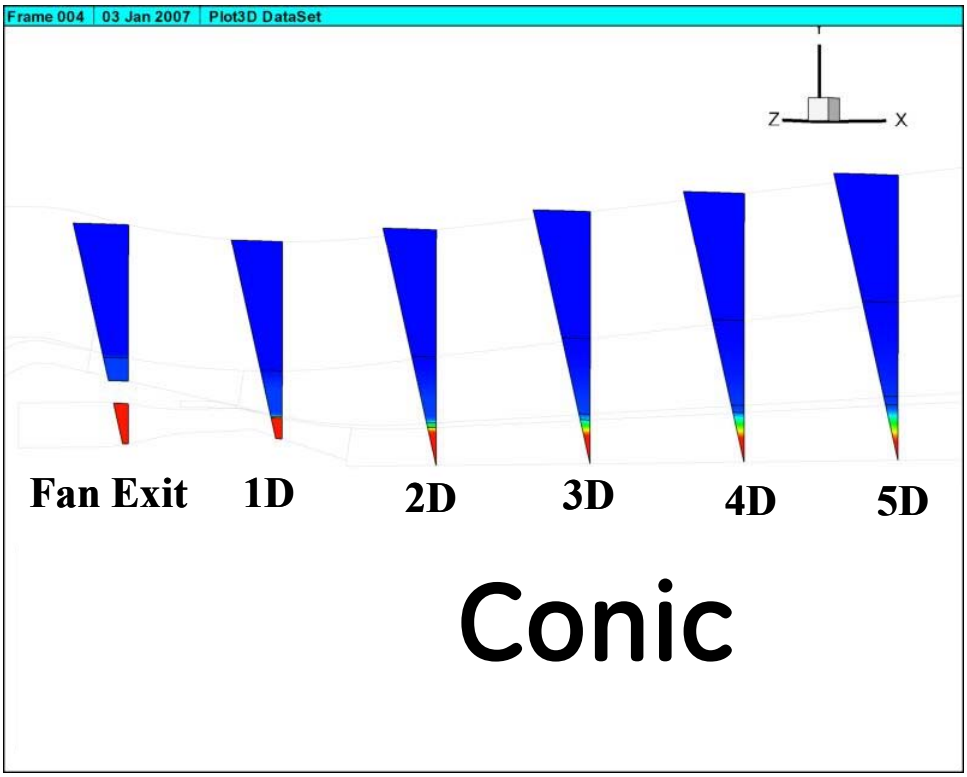

Figure 6. Jet Total Temperature Distribution Comparison

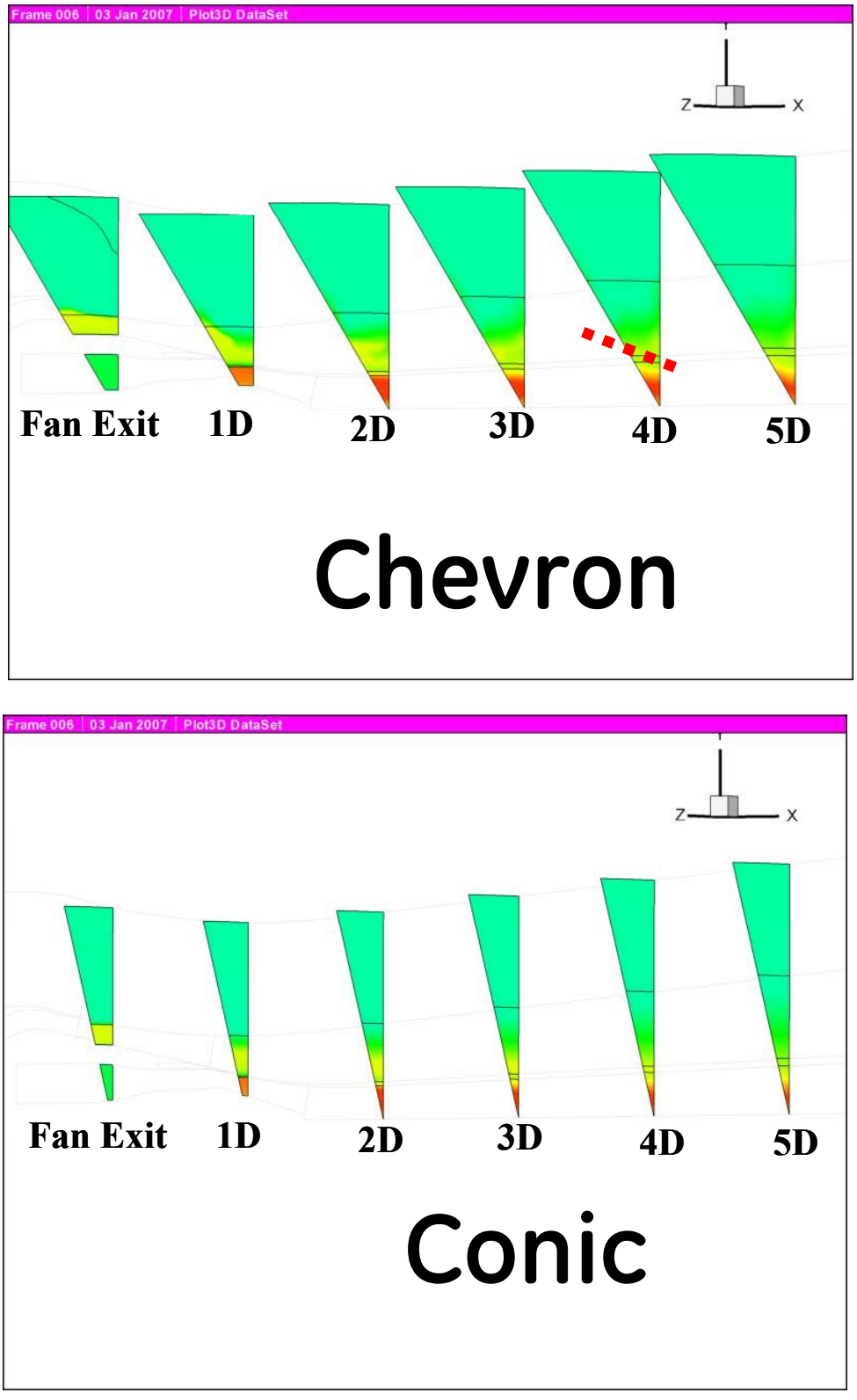

Figure 7. Jet Velocity Distribution Comparison

The results of the enhanced mixing are further demonstrated by the stream-wise evolution of the jet total temperature and velocity fields, which are presented for Case 12 in Figures 8 and 9, respectively. Figure 8 compares the jet total temperature evolution downstream of the conic nozzle to that for the chevron nozzle, along a plane intersecting the chevron tip. Physically, this plane would be expected to experience the highest vorticity, therefore exhibiting the most mixing. The region from four diameters to six diameters (4D to 6D), as highlighted in the figure, shows considerably lower total temperatures for the chevron nozzle, where the entire core region is green past 5D. In contrast, there is a substantial hot core evident with the conic nozzle, as evidenced by the red inner core color contour extending all the way out to 6D. Corresponding comparisons of velocity data are presented in Figure 9. These data exhibit a much stronger mixing region, as evidenced by the cross-stream extent of the downstream shear layer, which is highlighted by the brackets on the right hand side. Based on the mixing enhancement, without substantial TKE penalties, as demonstrated in Figures 5-7, the chevron configuration 12 was selected for fabrication and testing in Cell 41.

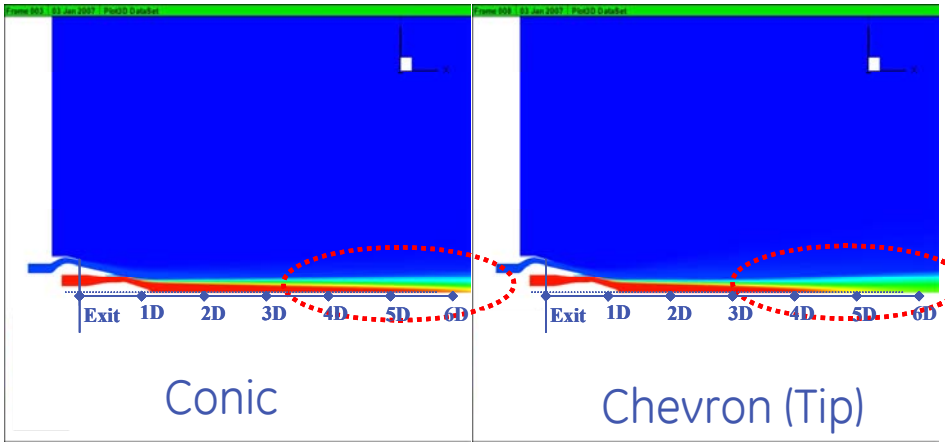

Figure 8. Compare Streamwise Evolution of Jet Total Temperature Profile

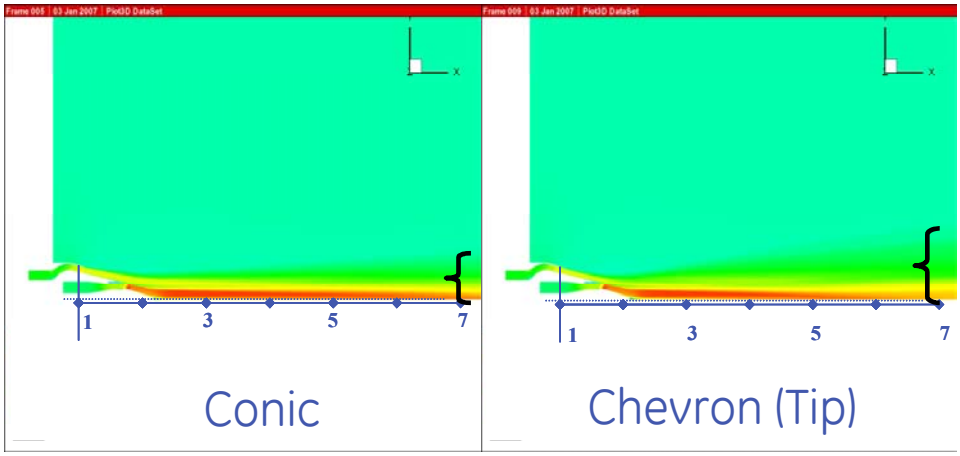

Figure 9. Compare Streamwise Evolution of Jet Velocity Profile

Similar analyses of the CFD predictions led to the selection of three new uniform fan chevron nozzles, Cases 6, 11 & 12 in Table 1. The final test matrix was also selected to assess the impact of chevron length, holding penetration constant (Case 6 vs Case 11), as well as the impact of chevron penetration, holding length constant (Case 11 vs. Case 12).

In addition to the uniform chevron nozzle designs, the experimental investigation was expanded to include two medium BPR azimuthally varying chevron nozzle test configurations. As noted in the prior quarterly reports, Subtask 3.3.4, which was originally planned to numerically investigate the effectiveness of medium BPR azimuthally varying chevron nozzles, could not be launched. Consequently, Subtask 3.3.2 was expanded to include two parametric variations on a uniform fan chevron nozzle, which exhibited typical fan chevron length and penetration values. Two azimuthally varying chevron nozzles were defined, based on the ”parent” uniform fan chevron nozzle design. Identical length distributions were defined for both azimuthally varying designs, such that the “average” chevron length was equal to the “parent” design. However, one of the azimuthally varying configurations was defined to give a medium “average penetration,” equivalent to the parent design, while the other was defined with low penetration. This was intended to provide a sense of the impact of penetration for an azimuthally varying design. Finally, in addition to the five new medium BPR fan chevron nozzle designs developed for this program, two existing chevron nozzles for the selected model were tested.

Testing

“Large-scale” model testing in the GE Jet Acoustics Facility at Cell 41 was performed in multiple phases, as outlined below. The first four phases were focused on the acoustic benefits of the potential designs. The last phase consisted of a limited series of cross-stream velocity measurements using the UC PIV system to qualitatively assess the mixing provided by the fundamentally different exhaust geometries. The sequential phases of the test were as follows.

1. Acoustic Benefit from Medium BPR Conventional Uniform Chevron Nozzles
2. Acoustic Benefit from Medium BPR Enhanced Mixing Technology Nozzles
3. Acoustic Benefit from High BPR Enhanced Mixing Technology Nozzles.
4. Acoustic Benefit from Medium BPR Azimuthally varying Chevron Nozzles
5. Cross-Stream PIV Measurements for Medium BPR Nozzles.

All of the acoustic data presented below were corrected for the refraction effects of the tertiary flow, prior to scaling. In addition, the data were also temperature-corrected, to account for test-to-test differences in the atmospheric attenuation, since Cell 41 is subject to seasonal variations in temperature and pressure.

As noted previously, UC supported the Cell 41 test in multiple ways. In terms of the overall testing, a UC student was present on site to assist with data collection and reduction for much of the testing, particularly during the new enhanced mixing technology development in Phases 2 & 3. In addition, the UC participant fabricated all of the enhanced mixing devices tested on both the UC and GE/Cell 41 hardware, and assisted GE technicians with installation on the Cell 41 models.

Phase 1 – Medium BPR Uniform Fan Chevron Testing

The existing medium BPR scale model exhaust nozzle was selected for this effort for two reasons: it's overall geometry was representative of current small commercial engine exhaust designs, and there were existing uniform fan and core chevron nozzles available for comparison to the new fan chevron designs, in addition to the conic/conic baseline. The configurations tested are shown below in Table 2.

Table 2. – Uniform Chevron Test Configurations

FAN NOZZLE			CORE NOZZLE	TEST DESIGNATOR
	CHEVRON GEOMETRY			
Type	*Length*	*Penetration*		
Conic	-	-	Conic	1111
Conic	-	-	Chevron	1110.01
#2 - Chevron	medium-short	medium	Chevron	1120.01
#3 - Chevron	medium-long	low	Chevron	1130.01
#4 - Chevron	medium-long	medium	Chevron	1140.01
#5 - Chevron*	medium	high	Chevron	1150.01
#6 - Chevron*	medium	medium	Chevron	1160.01

** - existing hardware*

Results of the acoustic testing of the conventional uniform chevron configurations are presented in Figures 10-12 below. All of the medium-BPR data presented in the following have been scaled to an appropriate full-scale size. Figure 10 shows the OASPL directivity pattern for all five uniform fan chevron nozzles, with a chevron core nozzle, as compared to the baseline conic nozzle. These data suggest that Test Configurations 1150.01 and 1160.01 were clearly the best designs. On an OASPL basis, the results indicate that all both are acoustically equivalent. However, corresponding spectral comparisons are presented in Figure 11, at a directivity angle of 140^{o}, which captures the peak jet noise levels. The spectral data indicate that Configuration 1150.01 provides similar benefit to 1160.01, but exhibits more high frequency lift. Of the candidate uniform designs, Configuration 1160.01 clearly provided the lowest high frequency penalty, nearly matching the high frequency levels of the baseline conic fan/chevron core configuration.

The overall EPNL benefits of each design are shown in Figure 12, for a nominal 1500 ft flyover at Mach 0.28. Again, Test Configuration 1160.01 clearly provided

the best jet EPNL benefit, with Test Configuration 1150 being similar, but not quite as good. The strong performance of Test Configurations 1150 and 1160 result is particularly interesting, they were based on Fan Chevron Nozzles #5 & #6 (see Table 2), which were existing designs for the selected test model. In contrast, Test Configurations 1120, 1130 and 1140 were based on Chevron Nozzles #2, #3 & #4, which were the new uniform designs based on CFD Cases 6, 11 & 12, above, that were developed specifically for this investigation. Prior tests of the existing hardware showed substantially less benefit, however, when coupled to a different pylon geometry. This suggests, as demonstrated recently by others, a strong dependence of fan chevron performance on jet/pylon interaction effects.

Finally, consider the test matrix of new nozzle designs, Test Configurations 1120, 1130 and 1140. These nozzles were specifically designed to investigate the relative impact of uniform chevron length and penetration. As shown in Table 2, Configurations 1120 and 1140 had the same penetration, with varying length, while Configurations 1130 and 1140 had the same length, with varying penetration. The EPNL data presented in Figure 13 indicates that Configuration 1140.01 was the best performing the new uniform nozzle design, despite exhibiting more high frequency penalty than 1130.01, which limited the EPNL benefits to higher speeds. The spectral comparisons in Figure 12 indicate that the low frequency benefit for 1130.01 was below that of the other two new designs, which suggests that the low frequency benefit with uniform chevrons may be more dependent upon penetration than length. Using a similar argument, the stronger high frequency penalty exhibited by Configuration 1120.01 as compared to Configuration 1140.01 (which was longer than 1120.01, with the same penetration), suggests that the high frequency penalty (or lift) associated with uniform fan chevron designs may be more dependent on chevron length than penetration.

Since they were the best performing new and existing nozzles, respectively, Chevron #4 and Chevron #6 (Configurations 1140.01 and 1160.01) were selected for comparison to the medium BPR enhanced mixing technology results, as well as the azimuthally varying designs below.

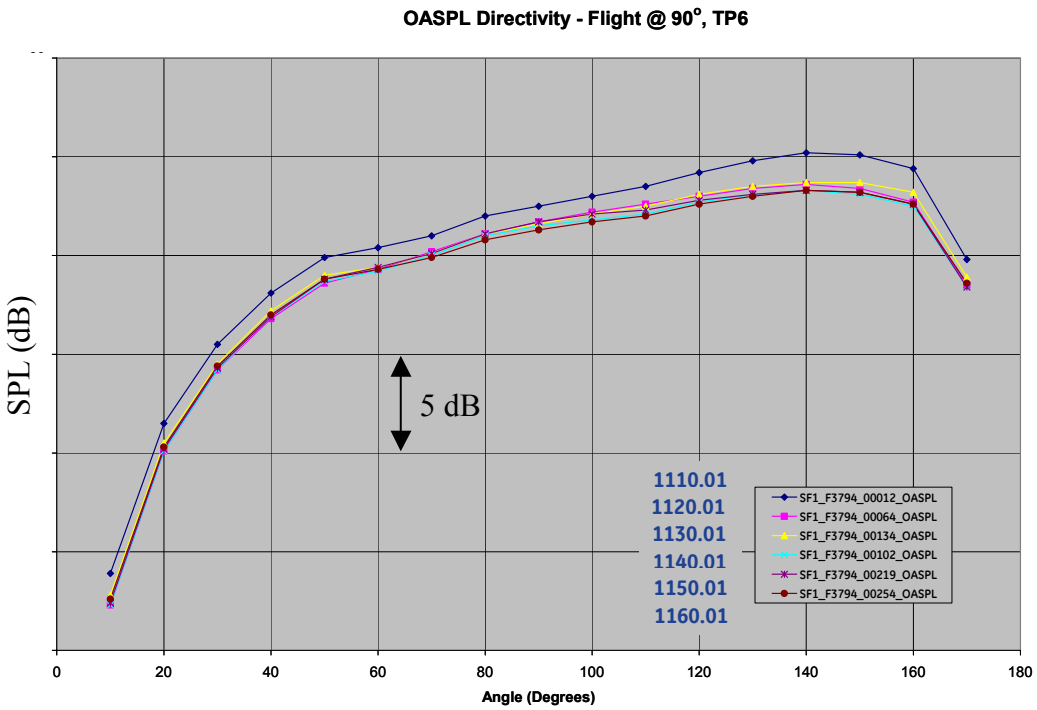

Figure 10. OASPL Directivity Comparison for Uniform Fan Chevron Nozzles

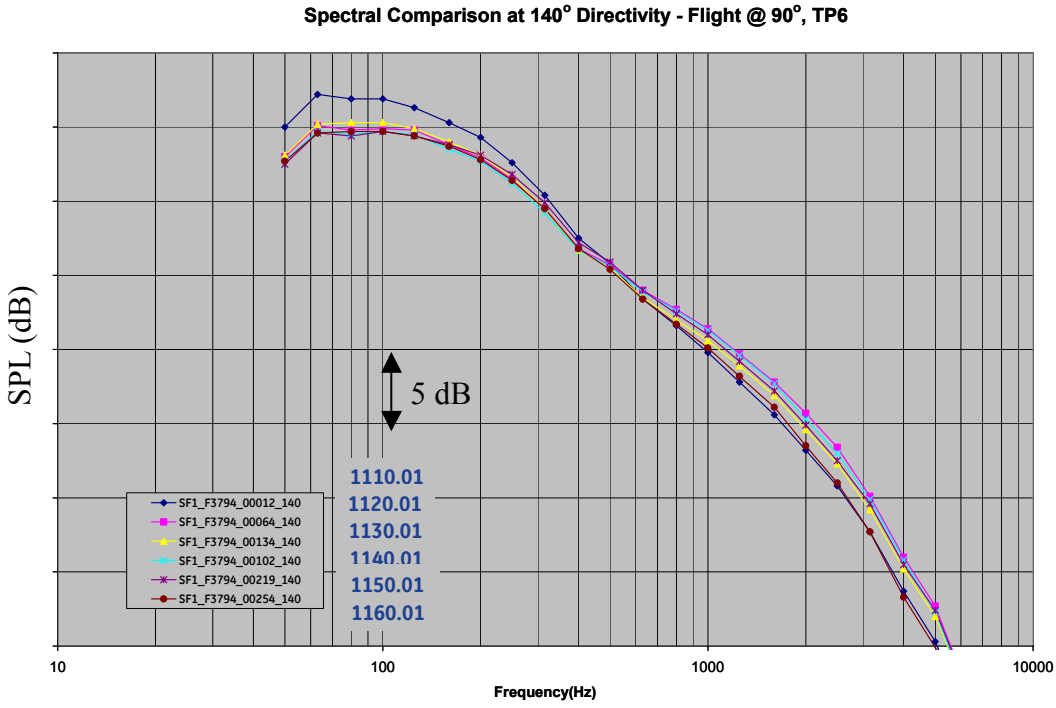

Figure 11. Spectral Noise Comparison at 140 deg. Directivity for Uniform Fan Chevron Nozzle Designs

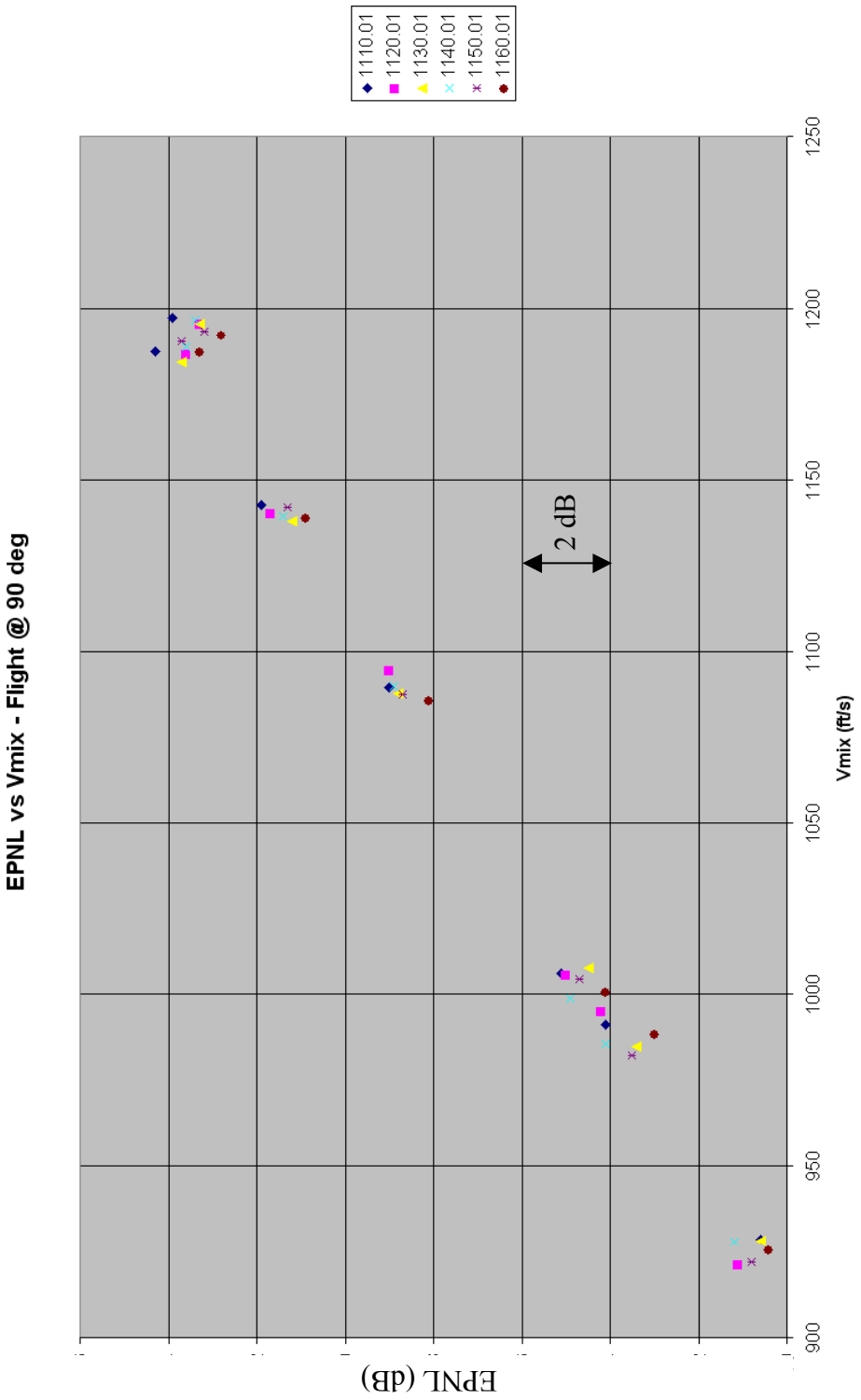

Figure 12. EPNL vs Mixed Jet Velocity Comparisons for Uniform Fan Chevron Nozzle Designs

Phase 2 – Medium BPR Enhanced Mixing Technology Nozzle Testing

In addition to the uniform chevrons, a series of new enhanced mixing technology concepts were tested on the medium BPR Cell 41 model. The initial geometries tested were scaled up from the optimal configuration identified in small-scale model testing at UC.

For the initial tests, the enhanced mixing technology devices were fabricated to provide an equivalent geometry to the UC design, scaled up to the selected Cell 41 medium BPR model. A series of different distributions of these devices were tested. The OASPL directivity comparisons presented in Figure 13 suggest that the results observed at UC were scalable, since all of the enhanced mixing configurations tested provided benefit on an OASPL basis. They also indicated that a particular distribution was optimal, relative to the other two. When the corresponding spectral data were examined, as shown in Figures 14 & 15, two features were striking. As expected from the OASPL results, a substantial low frequency benefit was achieved with all of the enhanced mixing configurations, which varied with distribution. However, there was clearly a significant high frequency lift penalty, which was very similar for all three initial enhanced mixing configurations tested.

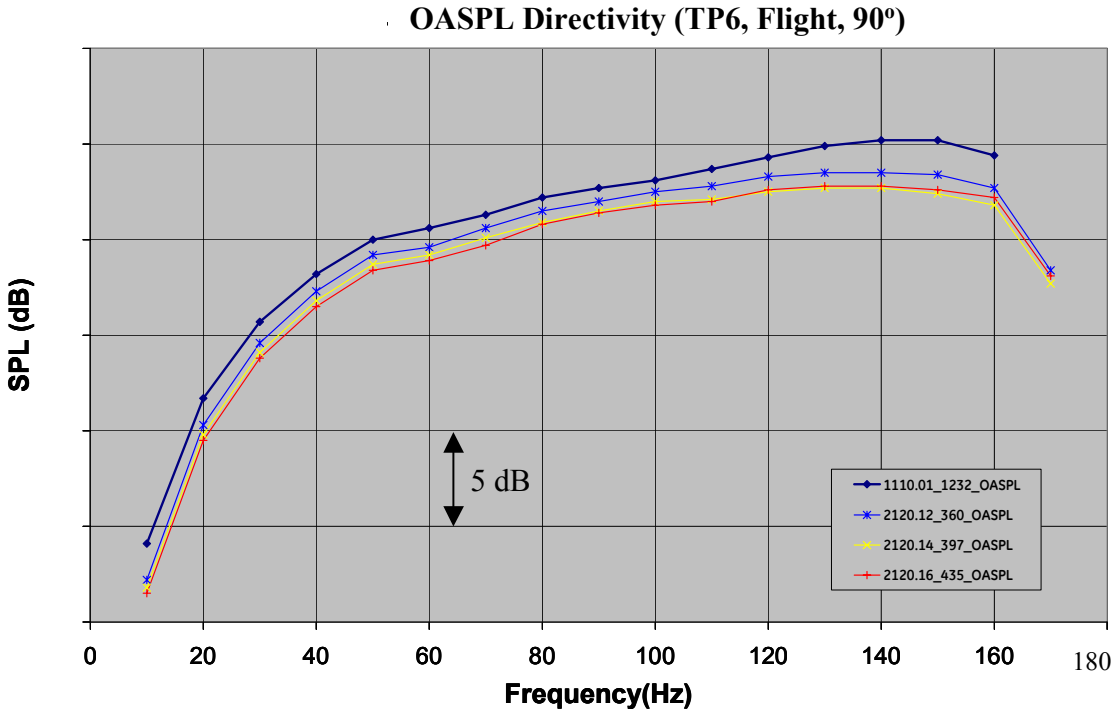

Figure 13. Initial Medium BPR Enhanced Mixing Technology Demonstration OASPL Benefit vs. Distribution

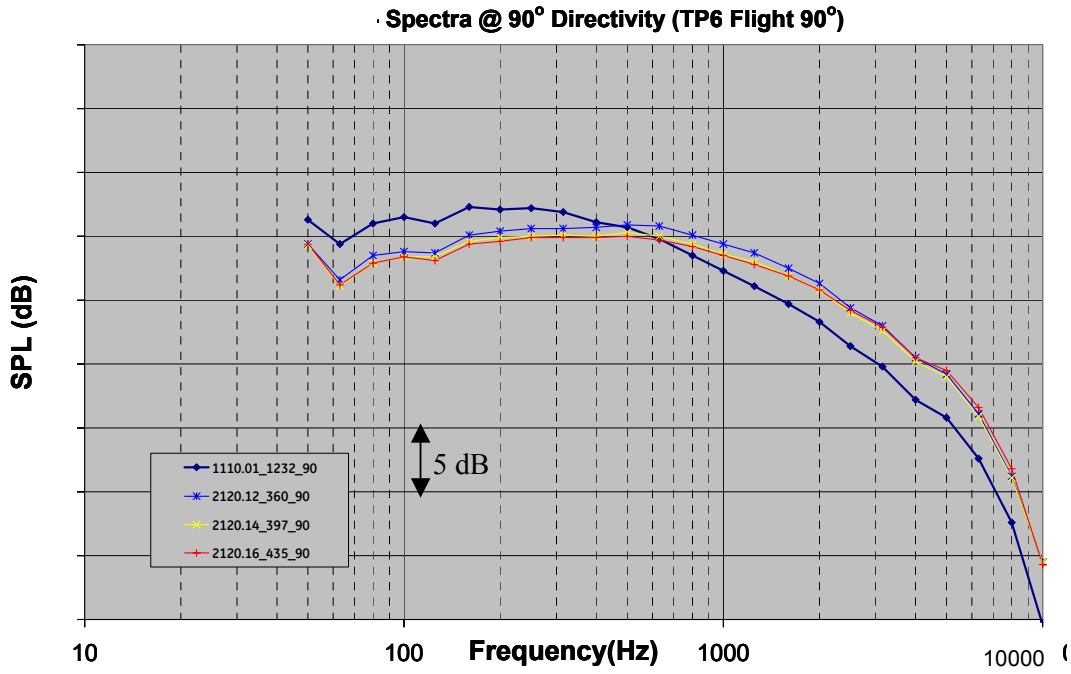

Figure 14. Initial Medium BPR Enhanced Mixing Technology Demonstration Spectral Acoustic Comparison at 90° Directivity

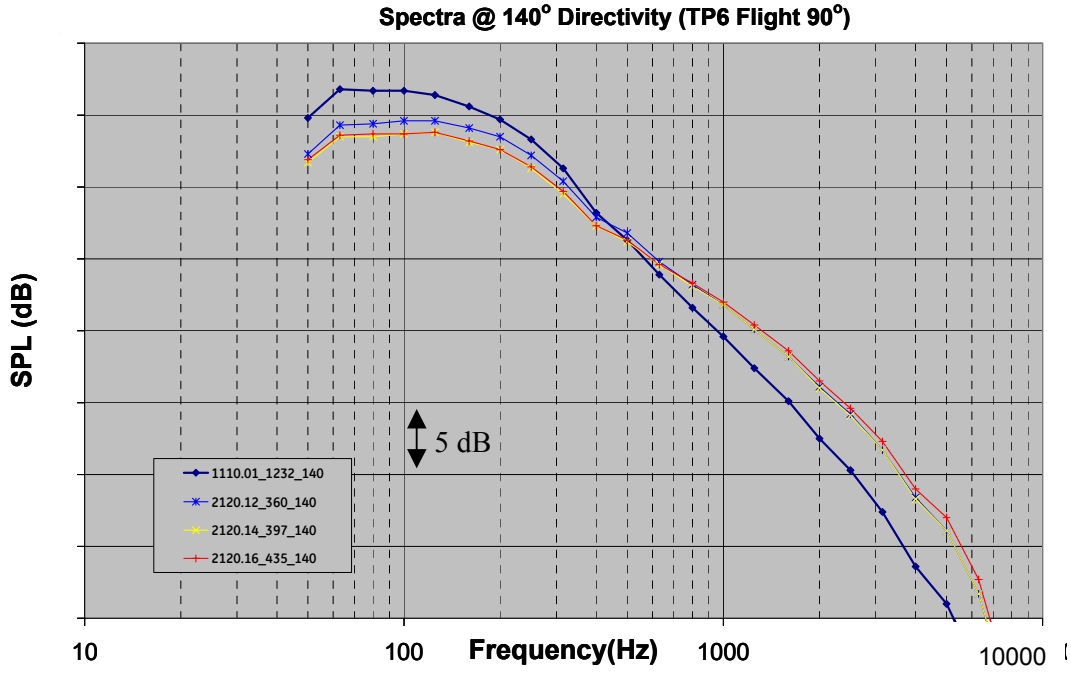

Figure 15. Initial Medium BPR Enhanced Mixing Technology Demonstration Spectral Acoustic Comparison at 140° Directivity

Once the acoustic benefit was verified in Cell 41 with the initial enhanced mixing technology distributions, the optimization of benefit with device geometry was investigated. Sample data are presented in Figures 16-18, below. All of the data presented here are for identical distributions of the enhanced mixing technology devices. Configuration 2120.14 refers to the "standard geometry" devices applied to a GE medium BPR model. However, Configurations 2120.64 and 2120.84 refer to modified geometries. Very little difference was noted in the OASPL levels, as shown in Figure 16. This suggested that the overall benefit had more to do with mixing technology distribution than device geometry. When the spectral data are considered, as shown in Figures 17 & 18, the overall benefit was similar because the low frequency benefit from all three configurations was essentially identical. However, the high frequency lift was substantially improved for some of the modified geometry cases.

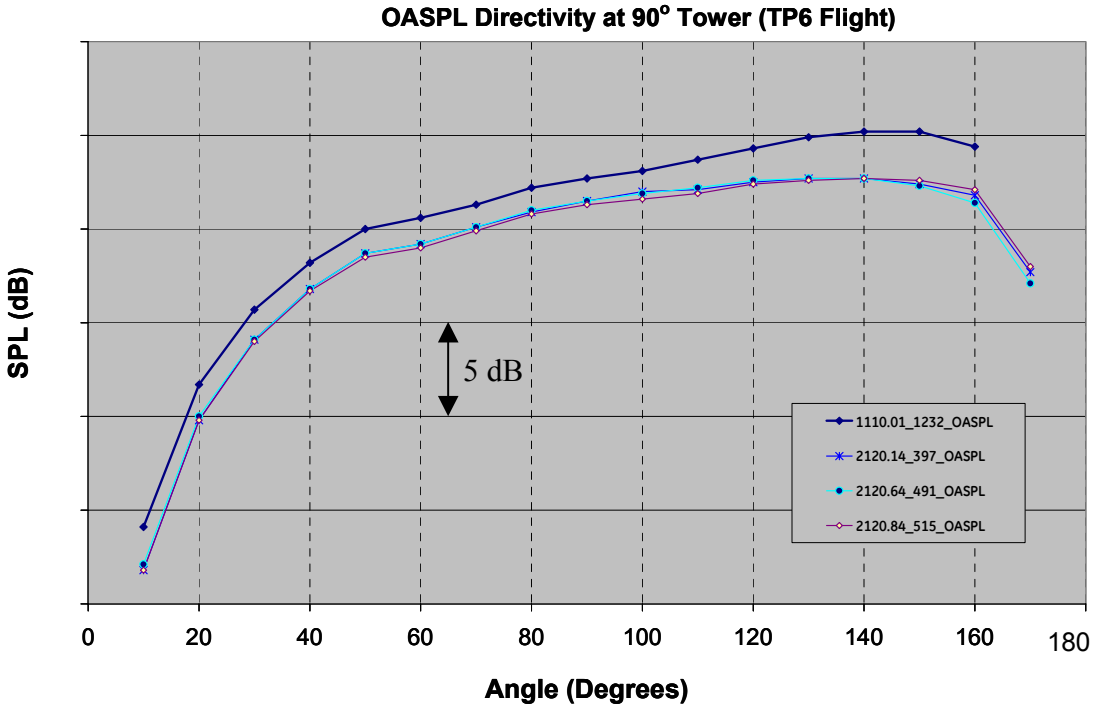

Figure 16. Medium BPR Enhanced Mixing Technology Demonstration OASPL Benefit vs. Device Geometry

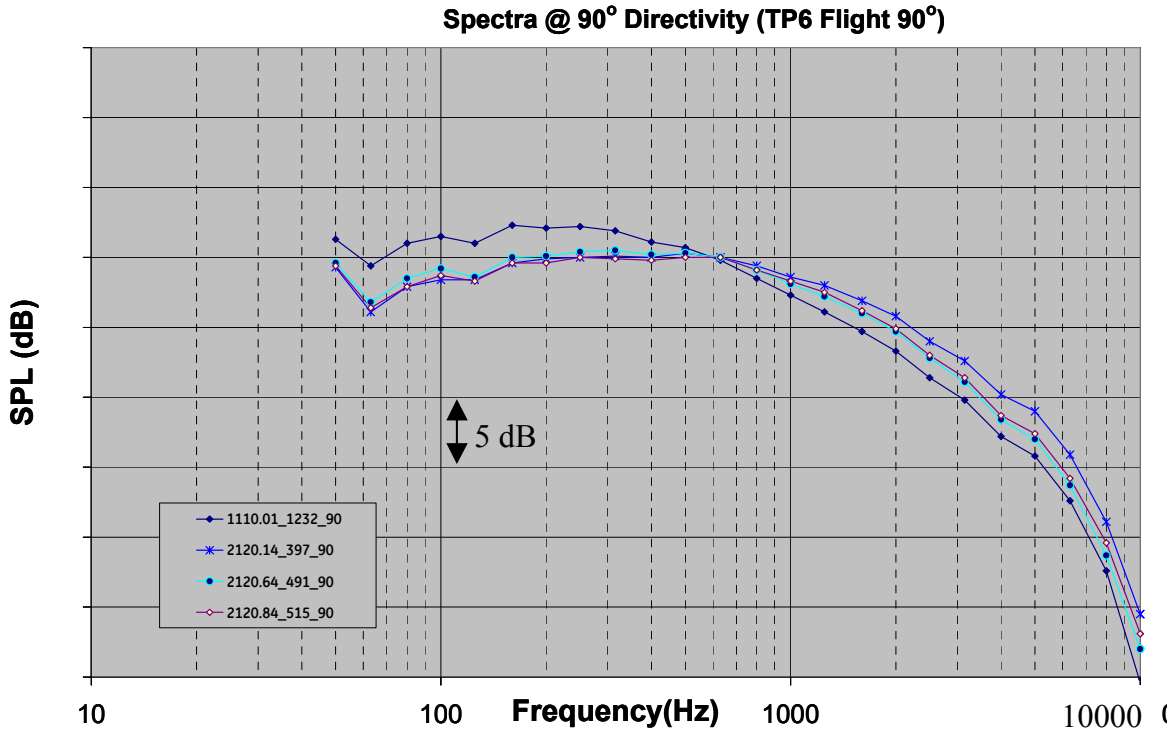

Figure 17. Medium BPR Enhanced Mixing Technology Demonstration Spectral Acoustic Benefit vs. Device Geometry at 90° Directivity

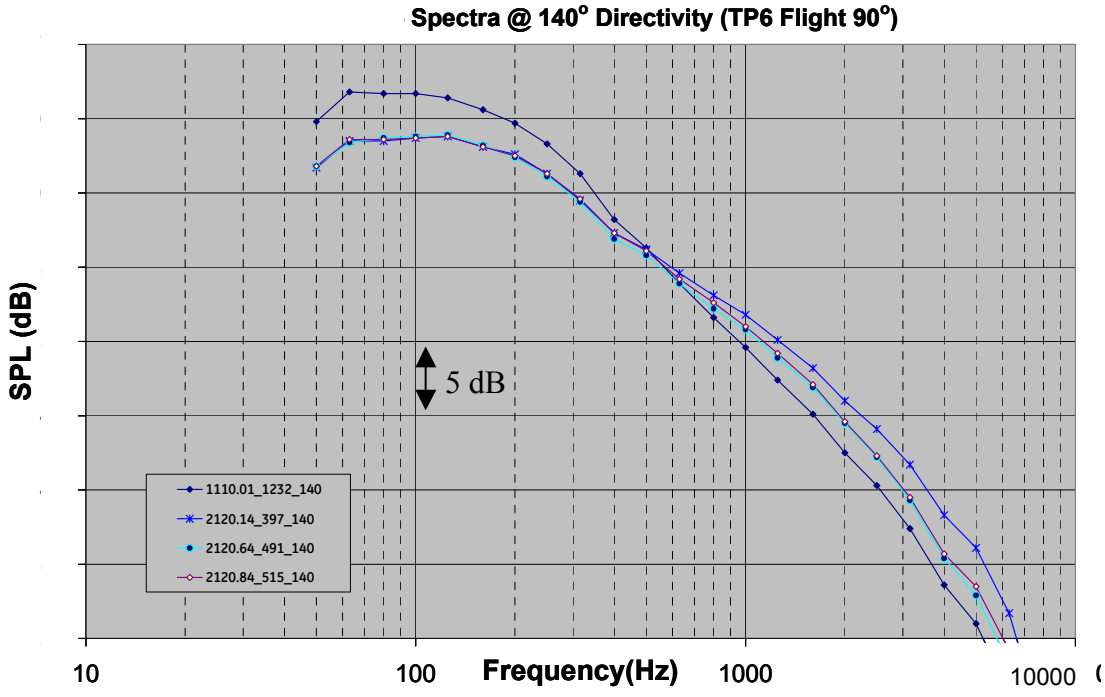

Figure 18. Medium BPR Enhanced Mixing Technology Demonstration Spectral Acoustic Benefit vs. Device Geometry at 140° Directivity

Finally, comparisons were made to assess the benefit of new enhanced mixing configurations relative to the uniform fan chevron nozzles tested above. These data are shown in Figures 19-21. In all of these figures, the data for three enhanced mixing technology cases presented above (Configurations 2120.14, 2120.64 & 2120.84) are plotted against the following: the conic fan/chevron core baseline (Configuration 1110.01); a conic fan/conic core reference (Configuration 1111); and the best new and existing fan chevron designs demonstrated in Phase II (Configurations 1140.01 & 1160.01).

Consider the OASPL comparison, presented in Figure 19. These data show a progression of benefits. The data for Configurations 1111 and 1110.01 illustrate the reduction due to the core chevron nozzle coupled to a conic fan, relative to a reference conic/conic configuration. This defines the baseline for the current fan nozzle test configurations. The two best uniform fan chevron designs clearly provide OASPL benefit relative to the baseline, with the 1160.01 providing slightly better performance at the jet-noise dominated aft angles, relative to the 1140.01. However, on an OASPL basis, all of the new enhanced mixing technology nozzles provided better performance than either conventional chevron design. Examination of the spectral data in Figures 20 & 21 illustrate that this additional benefit is due to 1-2 dB additional low frequency reduction with the new devices, despite some degradation in high frequency penalty.

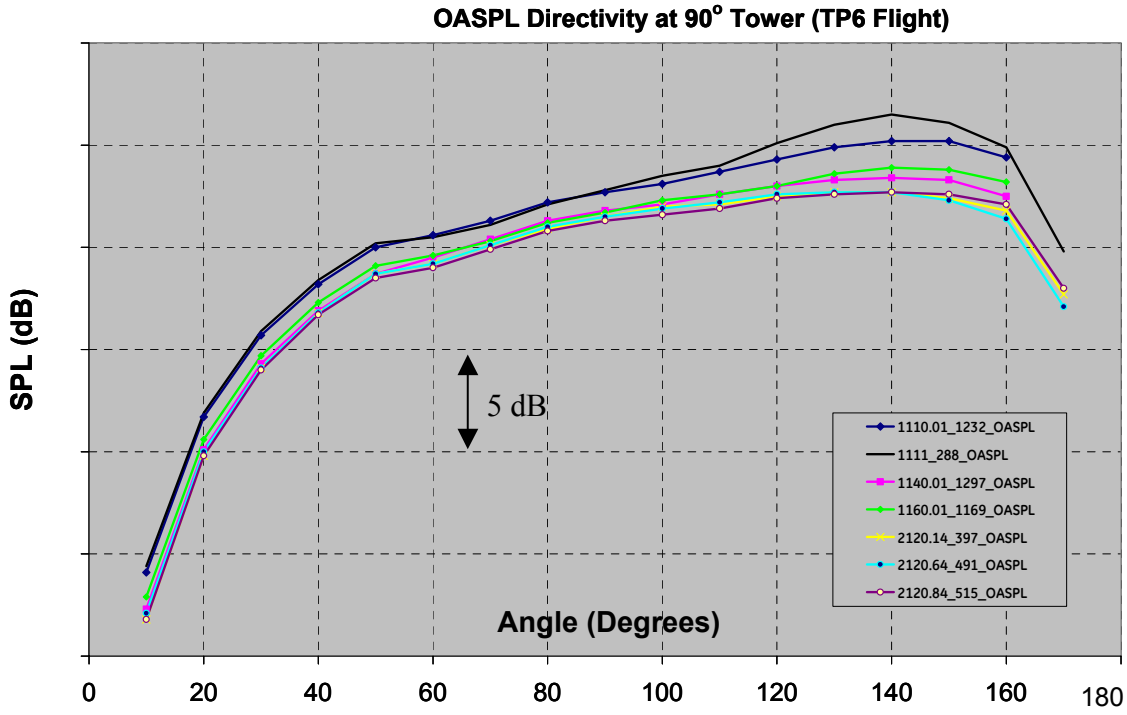

Figure 19. Medium BPR Comparison – Enhanced Mixing Technology Nozzle OASPL Benefit vs. Chevron

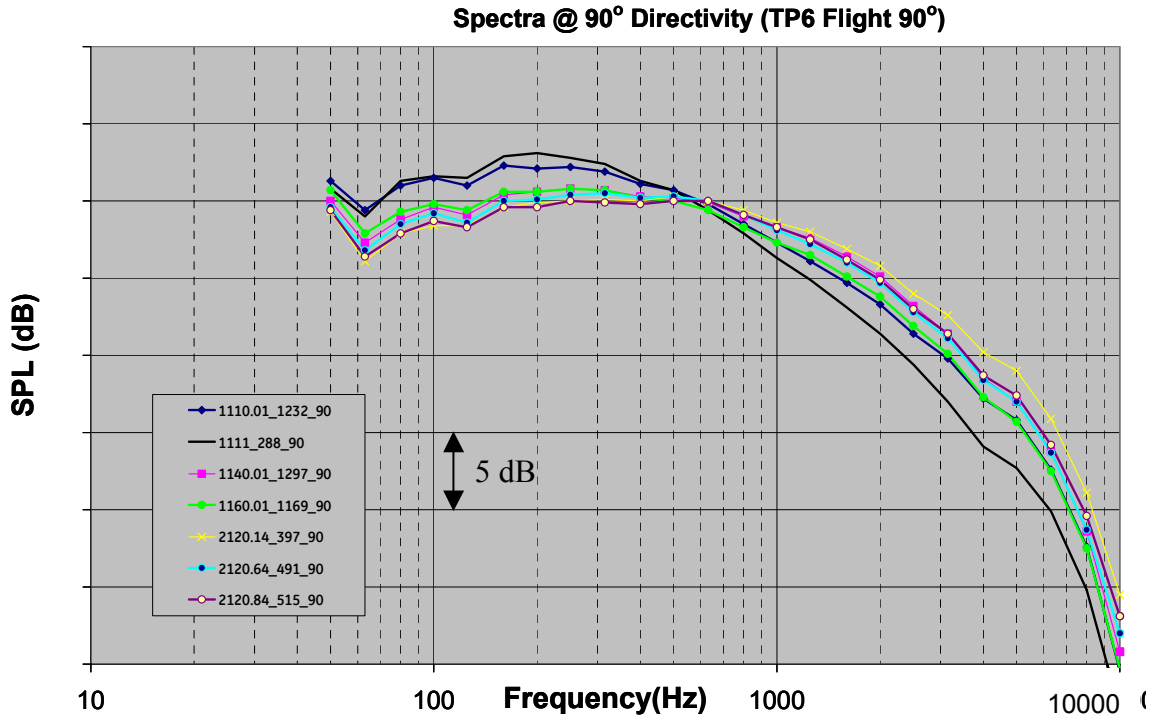

Figure 20. Med. BPR Comparison – Enhanced Mixing Technology Nozzle Spectral Acoustic Benefit vs. Chevron at 90° Directivity

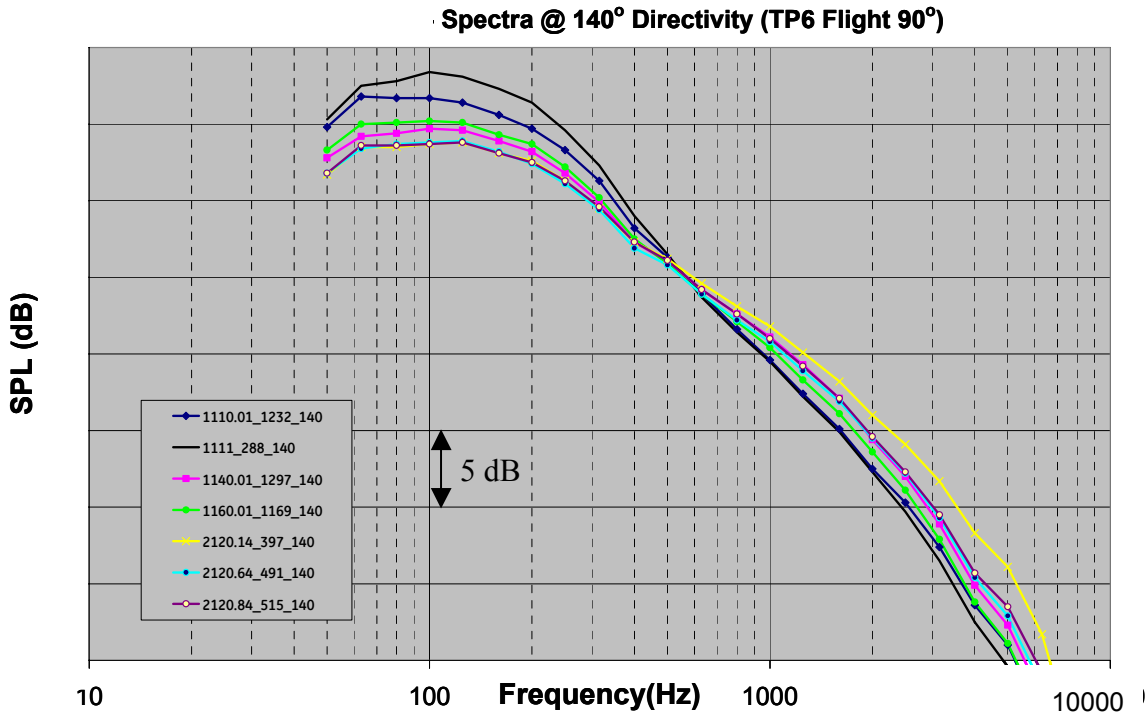

Figure 21. Med. BPR Comparison – Enhanced Mixing Technology Nozzle Spectral Acoustic Benefit vs. Chevron at 140° Directivity

Of course, for commercial applications, the bottom line acoustic impact is defined in terms of EPNL. In order to assess this, all of the model scale data were scaled up to an appropriate size for a small commercial engine. The scaled data were "flown" in a level 1500 ft flyover scenario, to estimate the EPNL levels that each configuration would achieve. These data are presented in Figure 22, below. In this plot, the baseline conic fan/chevron core (1110.01) and reference conic fan/conic core (1111) are plotted against the best new (1140.01) and existing (1160.01) uniform chevrons selected in Phase II. In addition, all of the reference enhanced mixing technology configurations (2120.12, 2120.14 & 2120.16) are plotted along with the modified geometry configurations (2120.64, 2120.84). These data suggest that two of the enhanced mixing nozzles, Configurations 2120.64 and 2120.84, both provided EPNL benefits similar to the fan chevrons, particularly at high speeds. There appears to be more degradation of the benefit at lower speeds with the new devices than the chevron nozzles. However, the strong degradation of acoustic benefit exhibited by the Configuration 2120.64, at the lowest speed is believed to be a bad data point, corrupted by background noise sources in the tunnel unrelated to jet noise.

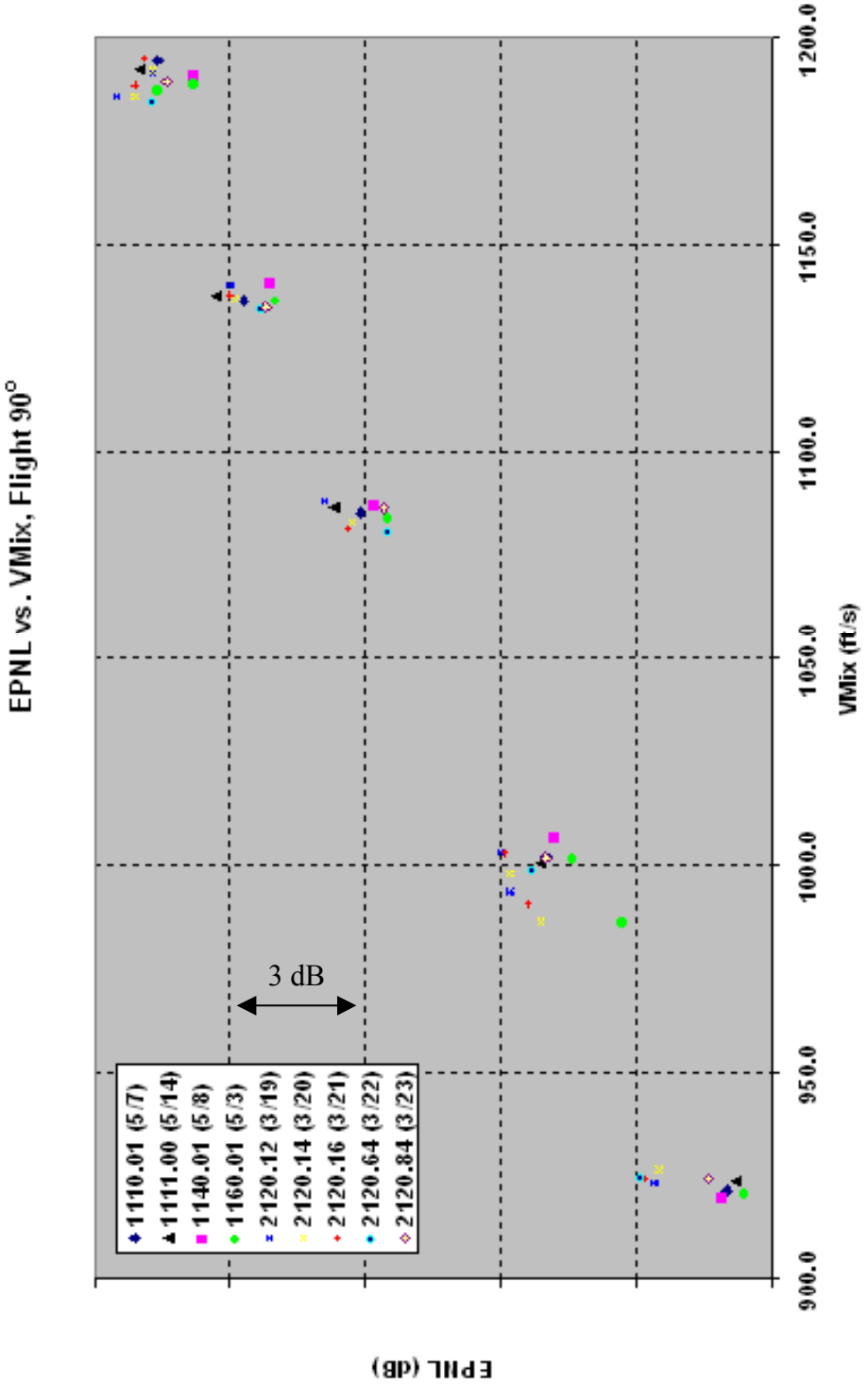

Figure 22. Med. BPR - EPNL Benefit of Enhanced Mixing Technology Designs vs. Uniform Chevron Nozzles

Phase 3 – High BPR Enhanced Mixing Technology Nozzle Testing

Since the new enhanced mixing devices were a new technology to be tested at the TRL 5/6 level in Cell 41, an existing high BPR exhaust model was selected, in addition to the primary medium BPR model, to assess the potential benefit for this technology on large commercial engine applications. A large number of device distributions and geometries were tested on the high BPR application, with mixed success. A select number of the enhanced mixing technology configurations tested are plotted in Figures 23-25, against a baseline conic fan/chevron core configuration (3110.01) and a reference conic/conic configuration (3111). On an OASPL basis, the data suggest that both the traditional fan chevron and the new enhanced mixing device configurations provide benefit relative to the baseline and reference configurations, as shown in Figure 23. However, close examination of the spectral data in Figures 24 & 25 shows that the low frequency benefit of both the conventional fan chevrons and the new devices is considerably smaller for the high BPR application than for the corresponding medium BPR applications in Phases 1 and 2. Furthermore, the high BPR application seemed to be more sensitive to high frequency degradation relative to the baseline conic fan/chevron core configuration. The high frequency lift exhibited by these sample configurations was significant, despite the fact that the geometries, relative to the "UC equivalent" scaled reference, were less aggressive than those successfully demonstrated on the medium BPR application in Phase 2.

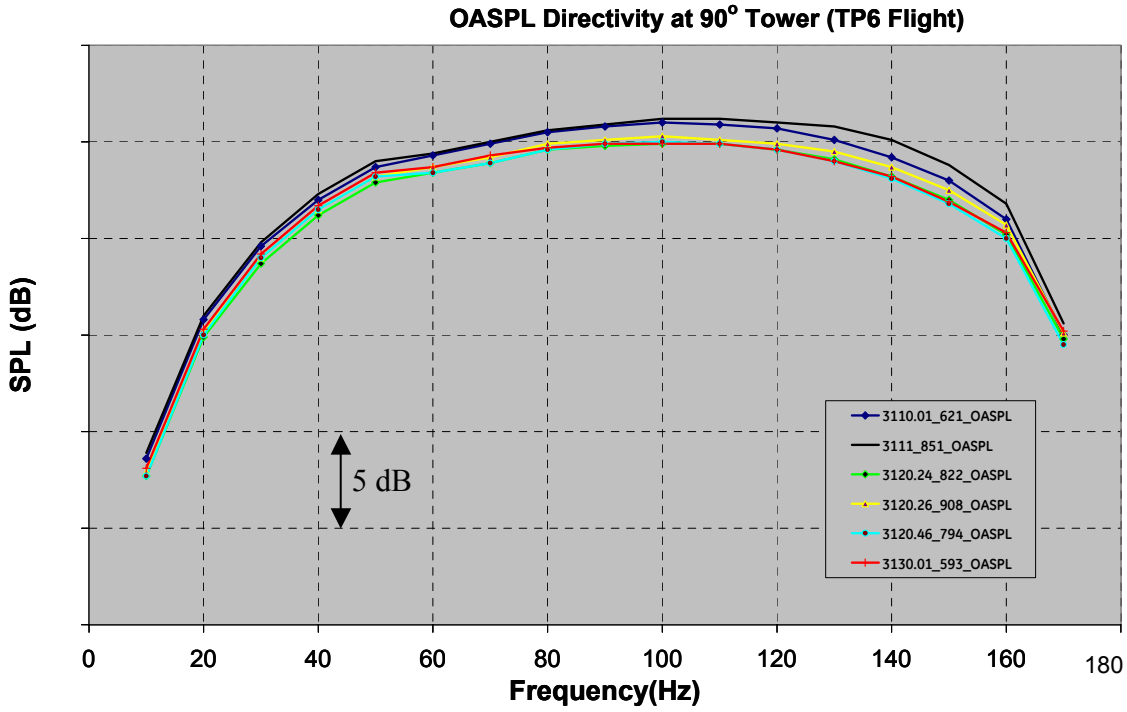

Figure 23. High BPR Comparison – Enhanced Mixing Technology Nozzle OASPL Benefit vs. Chevron

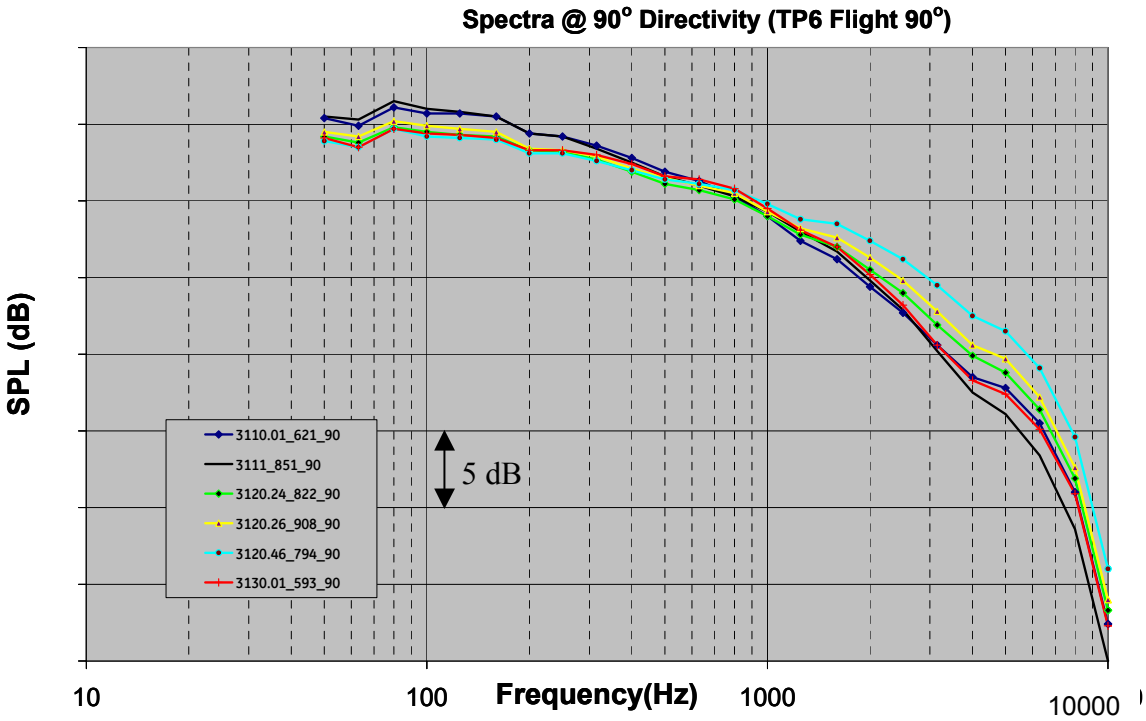

Figure 24. High BPR Comparison – Enhanced Mixing Technology Nozzle Spectral Acoustic Benefit vs. Chevron at 90° Directivity

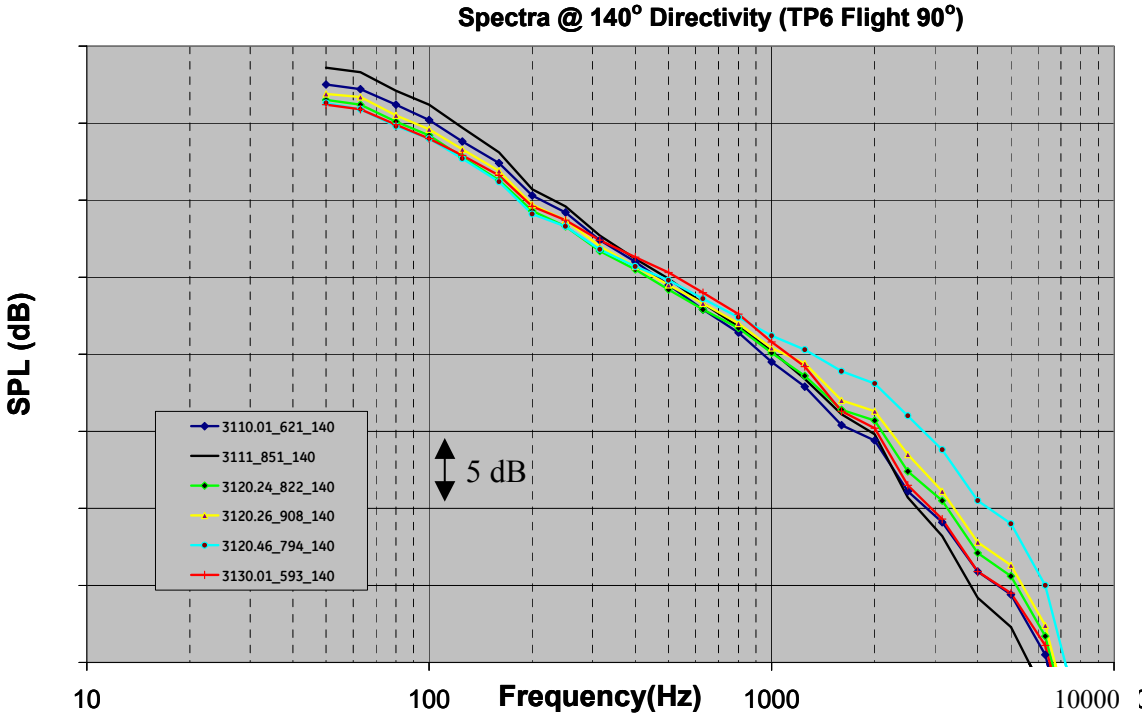

Figure 25. High BPR Comparison – Enhanced Mixing Technology Nozzle Spectral Acoustic Benefit vs. Chevron at 140° Directivity

As always, the bottom line acoustically was the EPNL impact. The high BPR data were scaled up to an engine size typical of a large commercial application and flown on a representative 1500 ft level Flyover trajectory to estimate EPNL. The results are presented in Figure 26. These data indicate that none of the fan nozzle technologies provided substantial EPNL benefits relative to either the baseline (1110.01) or reference (1111) configurations, except at the highest equivalent jet mixing velocity. At the maximum V_{mix}, two new technology configurations (3120.24 & 3120.26), showed small benefit relative to the baseline and reference configurations. Additional development is needed to optimize the designs for the low equivalent mixed jet velocities achieved with the high BPR cycle.

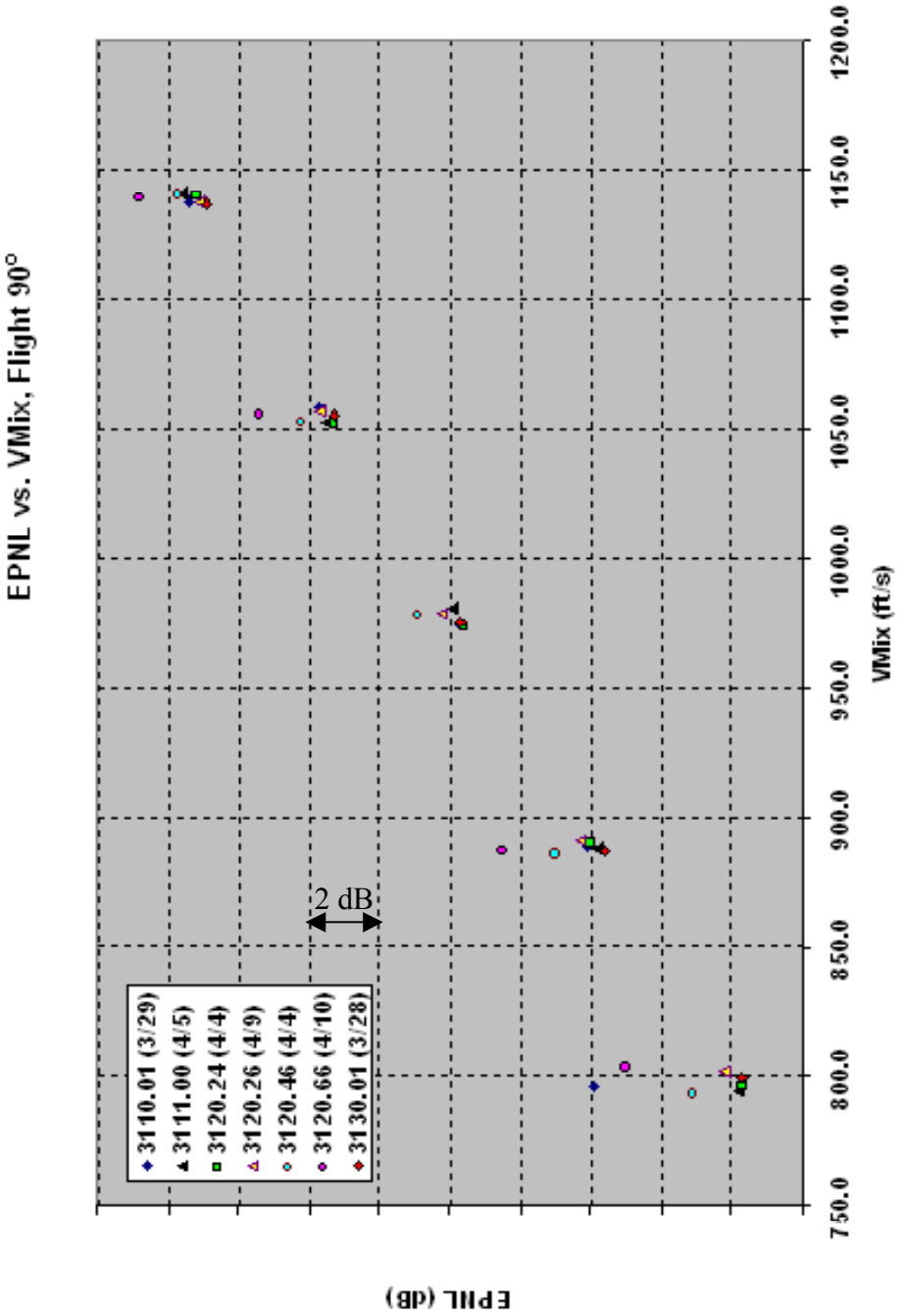

Figure 26. High BPR – EPNL Benefit of Enhanced Mixing Technology Designs vs. Uniform Chevron Nozzles

Phase 4 - Medium BPR Azimuthally Varying Chevron Nozzles

As noted in the previous quarterly reports, Subtask 3.3.4, which was originally planned to be a joint GE-NASA numerical investigation of the effectiveness of medium BPR azimuthally varying chevron nozzles, could not be launched. Consequently, Subtask 3.3.2 was expanded to include testing of parametrically defined azimuthally varying chevron designs. A ”parent” uniform chevron design was selected, with typical fan chevron length and penetration, on which two new azimuthally varying variants were based. The uniform chevron CFD design study suggested that fan chevron length governed the low frequency benefit, while the high frequency lift was linked to chevron penetration. To separately assess the impacts of these parameters, both azimuthally varying chevron configurations were defined with the length distribution, such that the “average” length corresponded to a typical fan chevron length. However, one azimuthally varying chevron nozzle was defined with a medium penetration (1170), while the other was defined with low penetration (1180).

Initial testing was performed to see how the acoustic benefit with the azimuthally varying designs compared to the best new and existing uniform chevron nozzles tested in Phase 2. Due to the azimuthally varying nature of the chevron geometry, substantial acoustic performance variation is expected relative to the pylon orientation. The Cell 41 test geometry is illustrated in Figure 27. The vertical orientation of the traversing microphone array is shown in part (a), while the relative circular motion of the traverse is indicated in the cartoon presented in part (b). The traverse tower angles at which the acoustic data were taken (8^o, 24^o, 60^o and 90^o) are indicated in Figure 27 (b) by the red lines. For acoustic testing, the model was assembled so that the 90^o tower location corresponded to 180^o from the pylon. Consequently, the observation angles, relative to the pylon were as shown in Table 3.

Table 3. Acoustic Observation Angles relative to Pylon

Acoustic Test Location	**Traverse Tower Angle (deg)**	**Observer Angle *relative to pylon* (deg)**
1	8	98
2	34	124
3	60	150
4	90	180

Table 4. Test Configurations for Phase 4,
Medium BPR Azimuthally varying Fan Chevron Testing

FAN NOZZLE				
	CHEVRON GEOMETRY			
Type	*Length*	*Penetration*	CORE NOZZLE	TEST DESIGNATOR
Baseline Conic	-	-	Chevron	1110.01
#4 - Uniform Chevron	medium-long	medium	Chevron	1140.01
#6 - Uniform Chevron*	medium	medium	Chevron	1160.01
#7 - Installation-Optimized Chevron #1	Varying	Medium	Chevron	1170.01
#8 - Installation-Optimized Chevron #2	Varying	Low	Chevron	1180.01

* - *existing hardware*

Initial acoustic comparison data for the azimuthally varying nozzles are presented in Figures 28-30, below. For simplicity, these initial comparisons focus on the 90^o Tower angle (180^o) from the pylon. The variation relative to pylon will be examined later for the best acoustic performing azimuthally varying configuration. In all three figures, the azimuthally varying design with medium penetration (1170.01) and the design with low penetration (1180.01) are plotted against the baseline configuration with a conic fan and chevron core nozzle (1110.01), as well as the best new and existing uniform chevron configurations tested in Phase 2 (1140.01 and 1160.01, respectively). The baseline and uniform chevron data are graphically depicted by thick lines (no symbols), while the azimuthally varying chevron results are represented by thin lines (with symbols). The low penetration design (1180.01) exhibited the best performance, so these tests were repeated. The results of both measurements are shown in Figures 33-35, showing excellent test-to-test agreement.

OASPL comparisons are shown in Figure 28. On an OASPL basis, both azimuthally varying configurations provide benefit relative to the baseline and uniform designs, away from the pylon. Corresponding spectral data are given in Figures 29 & 30, comparing the spectral acoustic content of all of the best fan chevron designs relative to the baseline at 90^o and 140^o directivity, respectively. The 90^o spectral data indicate that the low frequency benefit of both azimuthally varying configurations are comparable to the uniform chevron designs, but the high-frequency penalty associated with the medium penetration design (1170.01) approached that of the parent design (1140.01). In contrast, the results for the low penetration design (1180.01) exhibited much lower high frequency penalty, nearly on a par with the best performing uniform fan chevron nozzle (1160.01). In fact, the 140^o spectral data comparisons indicated that Configuration 1180.01 provided slightly more low frequency benefit, with less high frequency lift, than the best performing uniform nozzle at aft directivity angles.

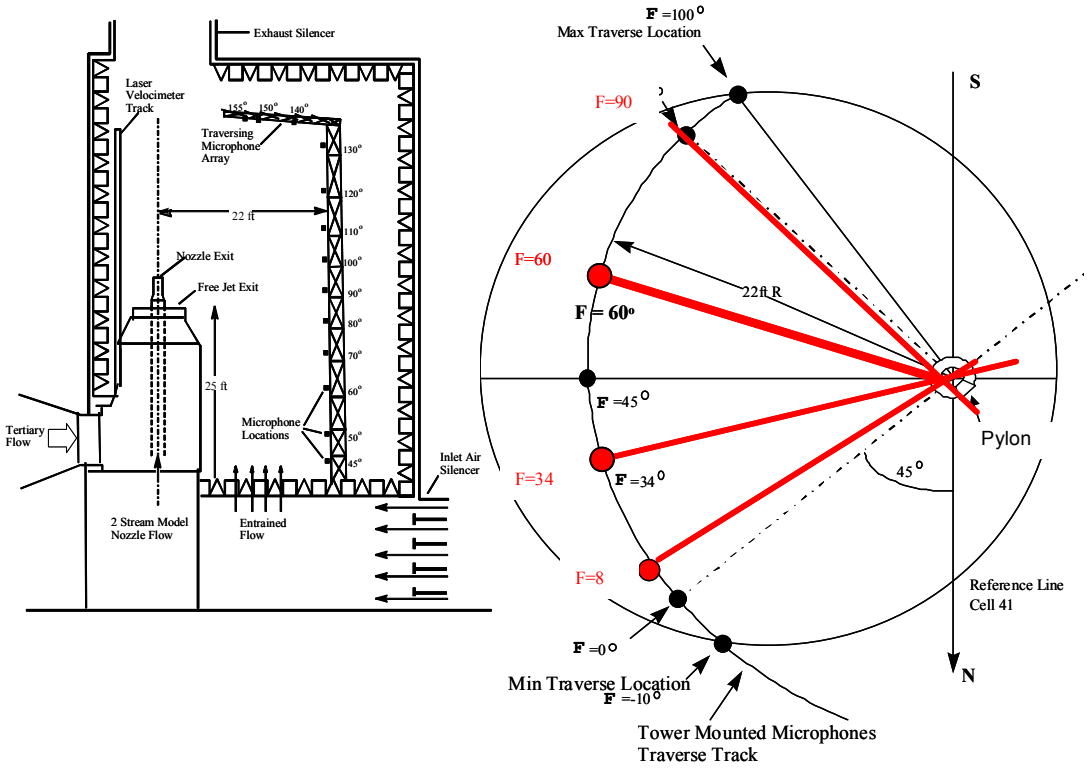

Figure 27. Cell 41Test Geometry

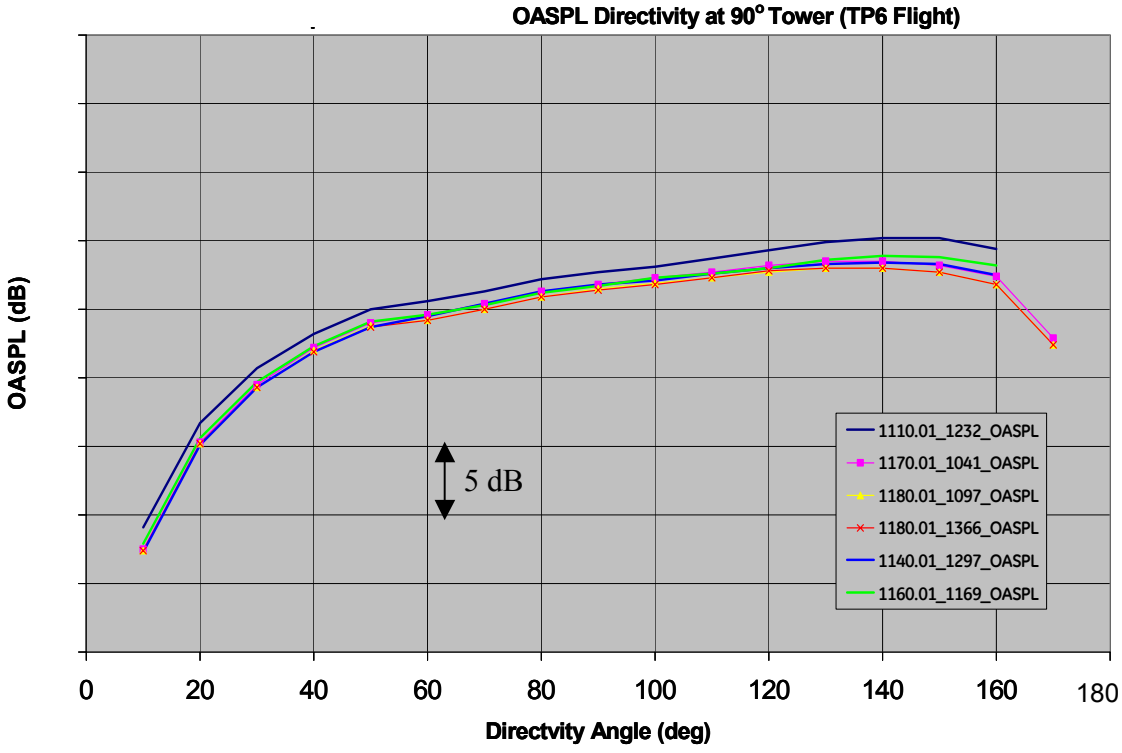

Figure 28. OASPL Comparison of Azimuthally varying vs Uniform Chevron Nozzles (180° from pylon)

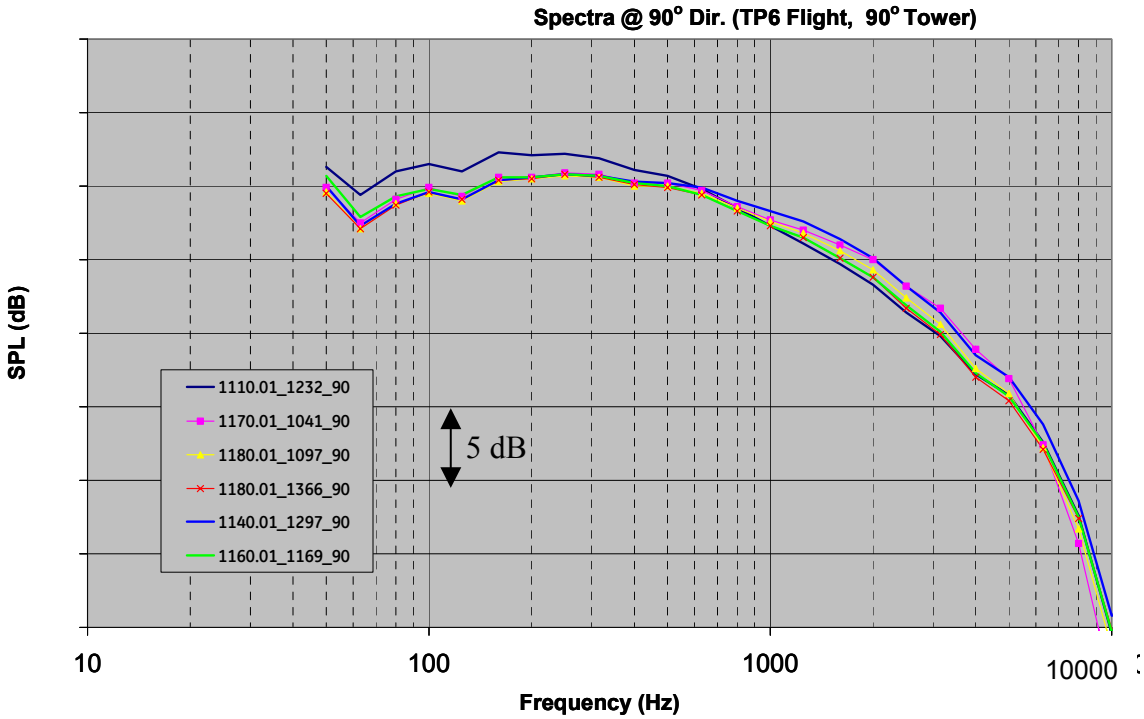

Figure 29. Initial Spectral Comparison of Both Azimuthally varying Chevron Nozzles vs Uniform Designs (at 90° Directivity, 180° from pylon)

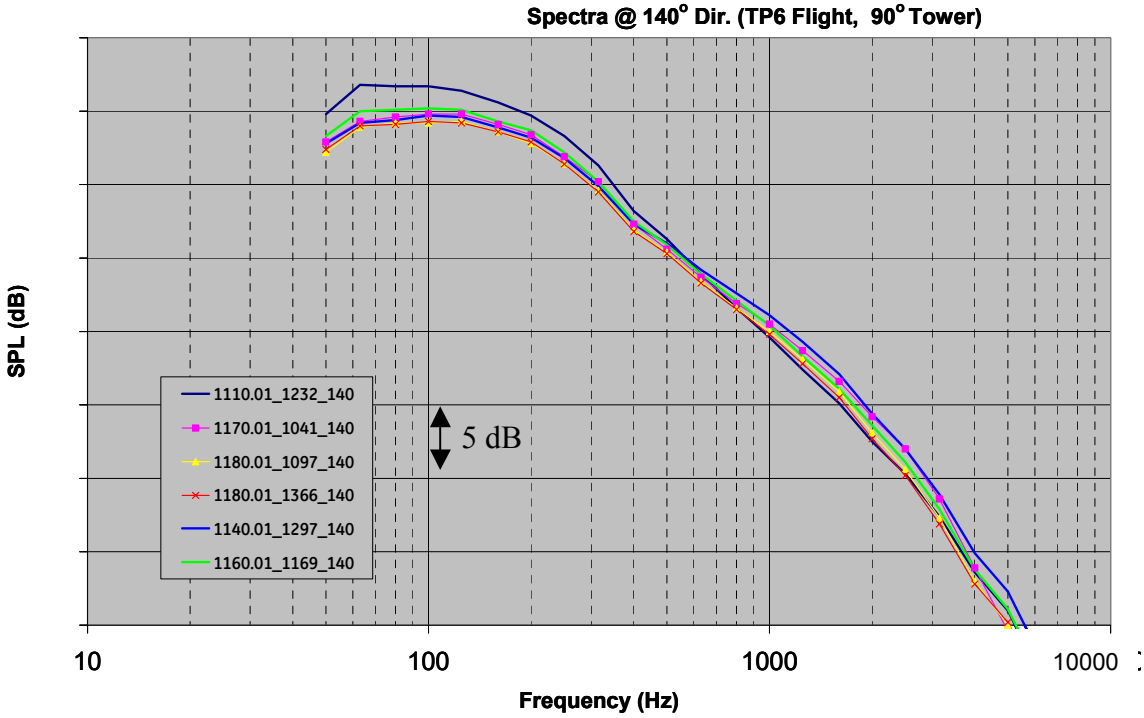

Figure 30. Initial Spectral Comparison of Both Azimuthally varying Chevron Nozzles vs Uniform Designs (at 140° Directivity, 180° from pylon)

The initial data comparisons presented above indicated that the low penetration azimuthally varying chevron nozzle (Configuration 1180.01) provided the most acoustic benefit of any medium BPR chevron nozzle tested. However, the azimuthally varying chevron design was expected to exhibit substantial variations relative to the orientation of the pylon. To characterize this effect, the variation of the measured acoustic levels for Configuration 1180.01 are plotted in Figures 316-33, for all of the observation angles listed in Table 3. For reference, these data are plotted against the nominal level for the baseline conic fan/chevron core configuration (1110.01), measured 180^o from the pylon (90^o Tower Angle).

The OASPL comparison in Figure 31 illustrates that the highest noise level, measured 98^o to the pylon, is roughly equivalent to the baseline configuration levels over the aft directivity quadrant, except at the far aft angles which still exhibit some chevron benefit. In the region from approximately 100^o-140^o, for the largest three Tower angles (34^o, 60^o & 90^o) the OASPL increase appears to track linearly with azimuth. However, at the lowest angle (8^o), this trend breaks down, exhibiting larger noise increases, relative to the observer angle, at the aft directivity angles. On the whole, the overall levels were no worse than the baseline configuration.

Next, consider the corresponding spectral data measured at 90^o Directivity as shown in Figure 32. These data suggest that the low frequency benefit is essentially the same for Configuration 1180.01 at all observation angles. The acoustic benefit variations are due to substantially different high frequency lift characteristics. At this directivity angle, there appear to be two different frequency bands in which the high frequency penalties are generated: 200-2000 Hz; and 4000-6000 Hz. The disparate values imply that two different physical scales may be involved, perhaps generated by two different high frequency sources.

Finally, the corresponding spectral data are presented in Figure 33 for 140^o directivity angle. These data do not exhibit separate high frequency penalties. Rather, the data for the 1180.01 configuration seem to smoothly transition from essentially zero penalty 180^o from the pylon to as much as a 7-8 dB broadband increase in the 500 Hz band 98^o from the pylon. Here, the broadband penalty stretches over all frequencies above 100Hz.

From a community noise perspective, the critical tower angles are 34^o and 90^o, since they correspond to the nominal source/observer geometry during at the Sideline and Cutback conditions. At 90^o, the benefit of the nozzle is clear, providing substantial low frequency reduction with essentially no high frequency penalty. However, at 34^o, the question is whether the high frequency lift outweighs the low frequency benefit exhibited in Figures 32 and 33. This leads to the final question in all of the acoustic comparisons, is there an EPNL benefit?

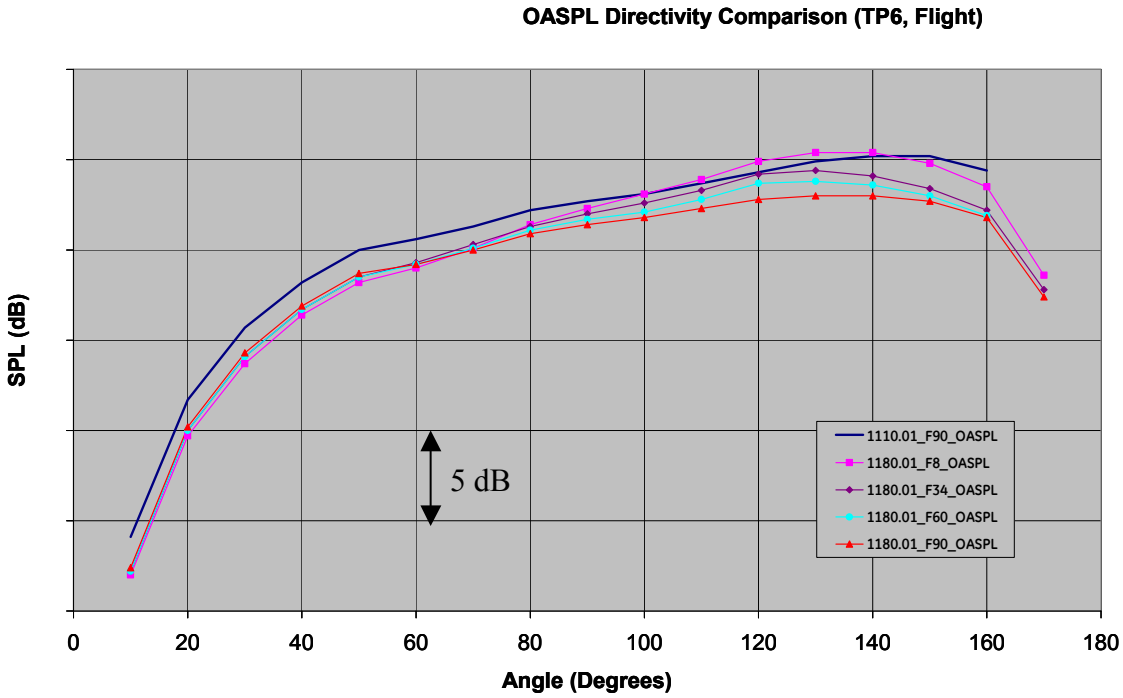

Figure 31. OASPL Variation Relative to Pylon Orientation Azimuthally varying Chevron vs. Uniform Designs (Flight, TP6)

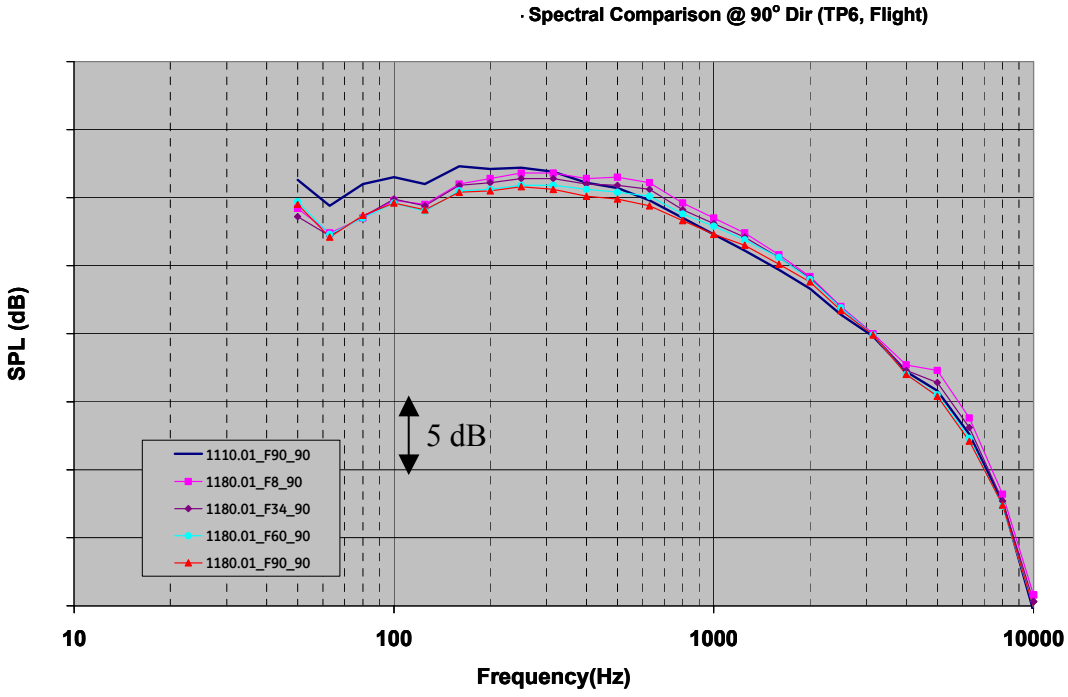

Figure 32. Spectral Variation Relative to Pylon Orientation Azimuthally varying Chevron vs. Uniform Designs (90° Directivity, Flight, TP6)

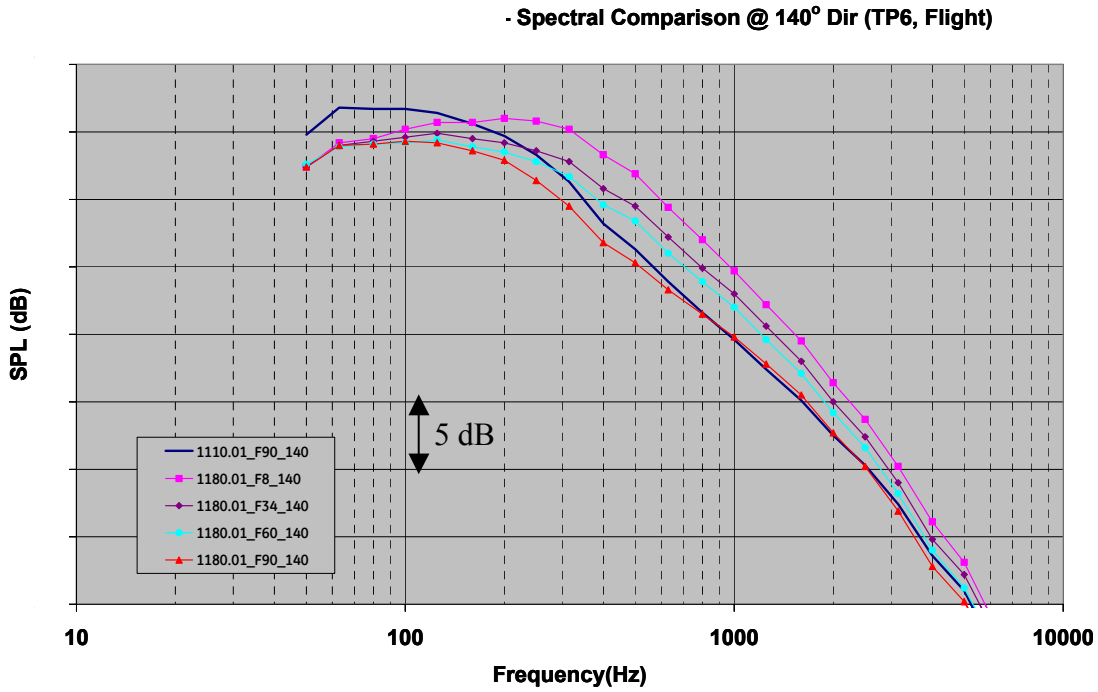

Figure 33. Spectral Variation Relative to Pylon Orientation, Azimuthally varying Chevron vs. Uniform Designs (140° Directivity, Flight, TP6)

As with the prior analyses, jet component EPNL estimates were generated based on a simulated 1500 ft flyover scenario. These data are presented in Figures 34 and 40, for the 90° and 34° tower angles, corresponding to the cutback and sideline geometries, respectively. For completeness, the EPNL comparisons are made for the baseline configuration (1110.01), two uniform fan chevron designs (1140.01 and 1160.01), and both azimuthally varying fan chevron configurations (1170.01 and 1180.01). Recall that, in Phase II, the best uniform chevron was 1160.01.

On the whole, Configuration 1170.01 provided no EPNL benefit, relative to the baseline, except at the highest speeds. This is attributed to the strong mixing that generated the high frequency penalty evident in the spectral data comparisons. However, Configuration 1180.01 provided substantially more EPNL reduction than any of the uniform designs at the highest speeds, with essentially the same benefit at lower speeds. It was the best chevron configuration tested on the medium BPR nozzle.

The primary outstanding design question remains the aerodynamic performance impact of this design. However, since Configuration 1180.01 was designed with low penetration, the aero performance impact would be expected to be minimal, relative to a typical uniform chevron design. A dedicated test is needed to quantify the aero performance impacts of the design.

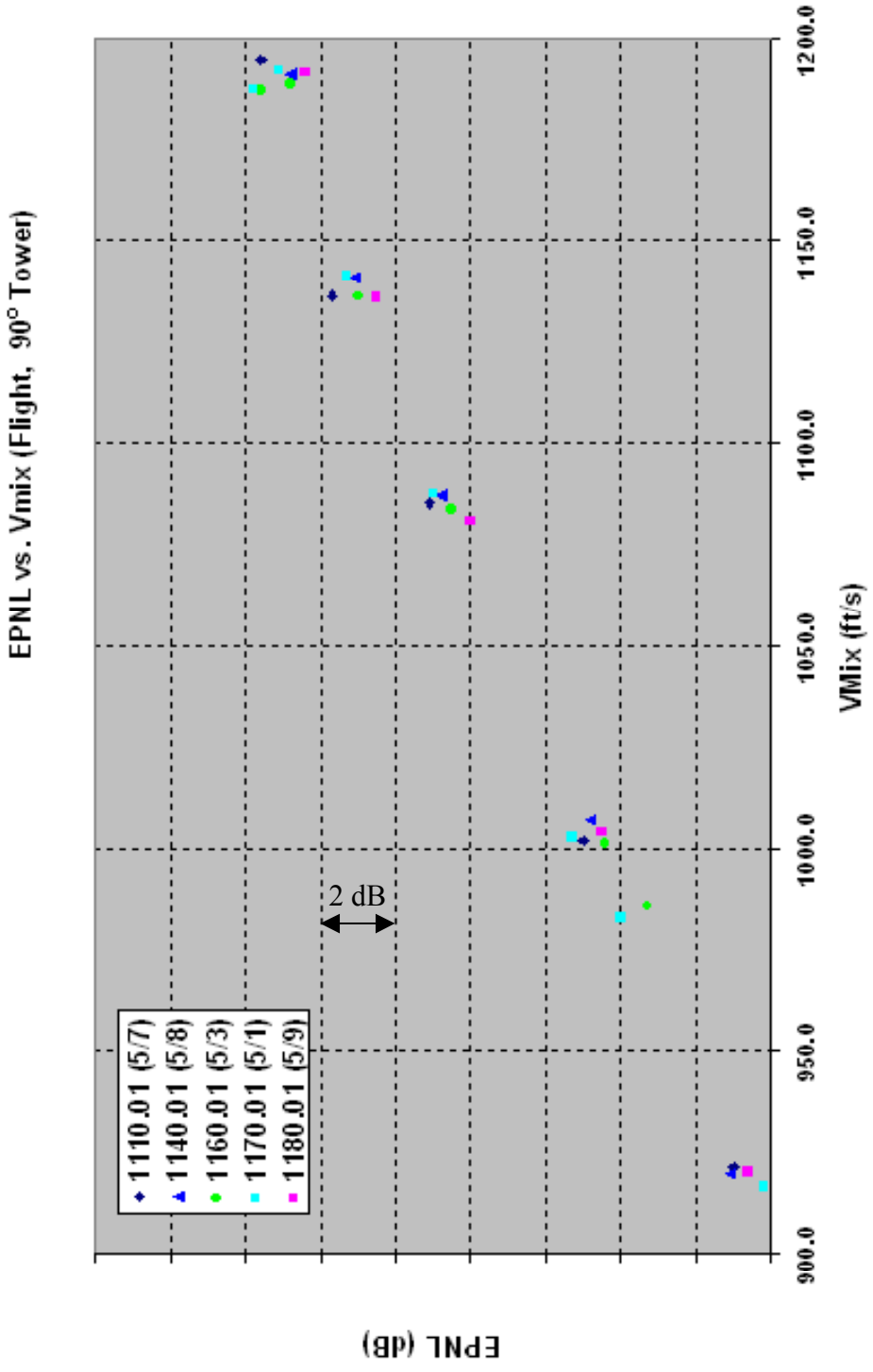

Figure 34. EPNL Comparison - Azimuthally varying vs. Uniform Chevron Nozzles (Flight, TP6, 90° Tower)

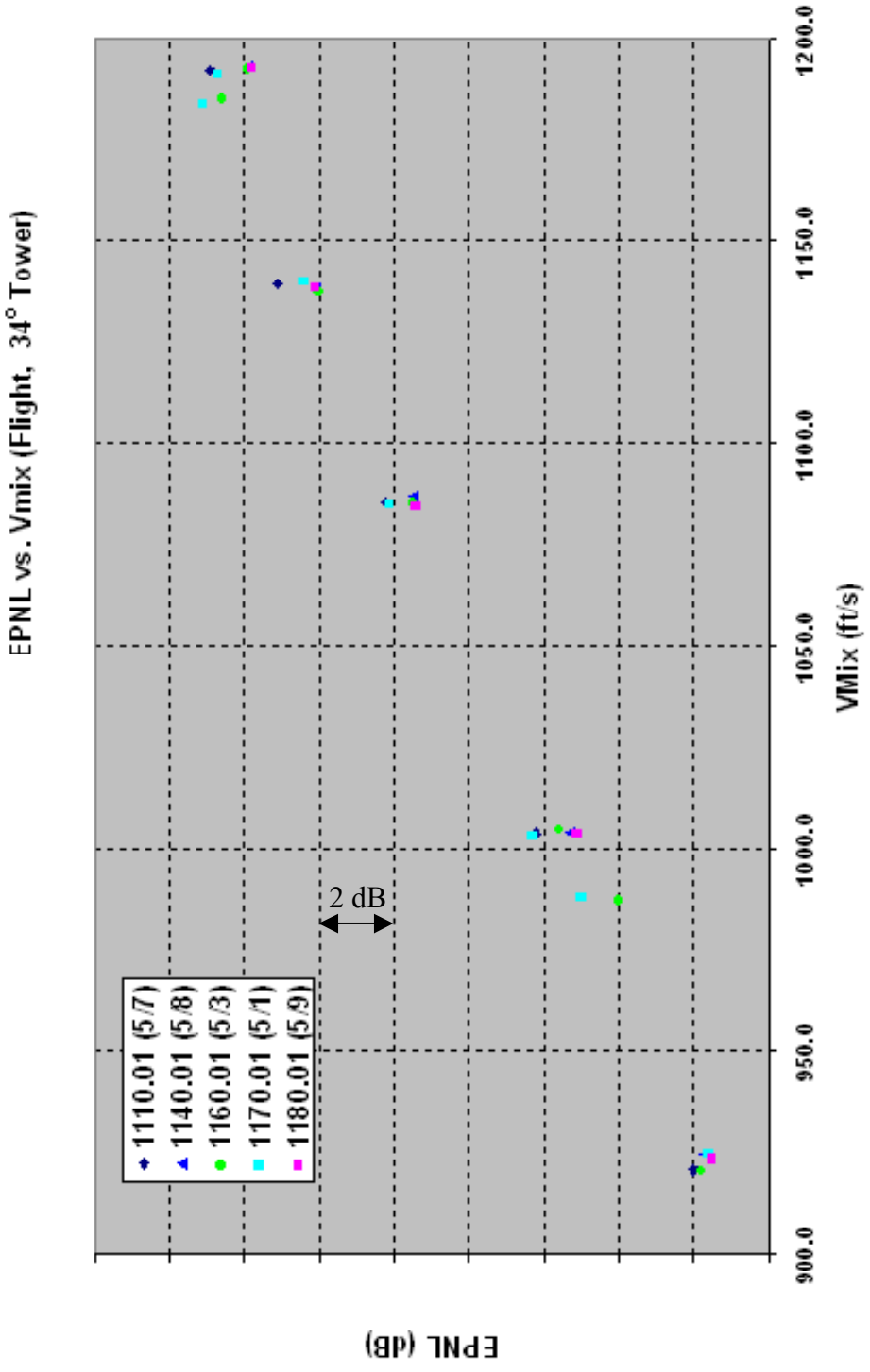

Figure 35. EPNL Comparison - Azimuthally varying vs. Uniform Chevron Nozzles (Flight, TP6, 34° Tower)

Phase 5 - PIV Measurements on Medium BPR Exhaust Nozzles

As noted below, Task 3.3.3, the development of a variable geometry exhaust nozzle bench top demonstration, was performed as a joint effort with Spirit Aerostructures Inc., and Continuum Dynamics Inc, where each organization provided their own resources. The funding that was originally allocated to that effort was re-allocated to a set of velocity measurements behind some of the successful medium BPR nozzle treatments. The velocity data were taken using a Stereo Particle Image Velocimetry (PIV) system, so that the flow distribution could be characterized over the entire field of view of the camera system, rather than using traditional Hot Wire or Laser Doppler Anemometry, which only provide point velocity measurements. Special thanks to the University of Cincinnati, for providing and operating the PIV system on site at Cell 41 in support of this effort.

Since this was the initial demonstration of PIV in Cell 41, there was no existing mount hardware for the laser or cameras. Instead, the cameras were supported by a work platform that fits over the test model in the cell. However, the floor of the platform obstructs the tertiary flow duct, so all of the measurements presented here are for static conditions (zero tertiary flow). In addition, the existing Cell 41 traverse system was too far from the model, and not precise enough, to position the light sheet, so all measurements were restricted to a single plane, approximately 0.4 inches above the tip of the model core plug.

The critical requirements for PIV are the illumination of the field of view, and sufficient seed density to resolve the flow structures. To measure the impact of an enhanced mixing exhaust nozzle, the flow in the fan/ambient shear layer must be resolved. However, since this was the first application of PIV measurement technology in Cell 41, initial measurements were made on the core exhaust nozzle. The core/fan shear layer was expected to be easier to resolve with the existing Cell 41 in situ seeding system, which seeds both the fan and core streams, but not the external flow. In fact, a supplementary external dry seeder, provided by UC, was also needed to ensure sufficient seeding in the fan flow. Finally, the number of images for each test point was limited to 200, making it difficult to solve for higher statistical quantities such as the Turbulent Kinetic Energy (TKE). However with 200 images, gross features appear that can be explored to provide some insight into the physics of the mixing.

Variation with Test Conditions

Consider the velocity contours presented in Figure 36 for the baseline conic core nozzle, at three different operating conditions (see Table 4). Although the actual peak velocities differ, as shown in Table 4, there are many similarities between all of the contours. Starting from the center of the jet, the presence of the center body leads to a low velocity in this region, since the measurement plane is just downstream of the plug tip. Moving away from the jet center, the flow speed

increases until the region of the core stream where the maximum velocity for this jet is found. Outside the core is a strong shear layer between the core stream and the fan stream, which is indicated by the rapid transition to the slower, larger, fan stream. Finally, external to the fan stream is another shear layer between the fan flow and ambient conditions. This is evident in the concentric blue circles on the right and left sides of each part of Figure 36. Another common feature is the existence of a slow region at the bottom of each contour (from Y = -40 to –60 mm, Z = 0). This feature is an artifact of the lower bifurcation in the model, whose wake defect effectively slows the flow in this region.

In addition to the contour plots, which are spatially illustrative, absolute and relative velocity comparisons were made along a given radial cut line, for all of the operating conditions. Figure 37, part (a) shows a contour plot for a high speed condition, with a black line indicating where a radial slice has been taken. The two line plots in parts (b) and (c) compare the streamwise velocity profile along this radial cut line. Part (b) compares the absolute magnitude, which agrees very well with ideally predicted velocities based on measured test conditions. Part (c) shows the profiles normalized by the core velocity. These data indicate that the relative velocity differential across the core/fan stream interface is larger with increasing test point, resulting in a stronger shear gradient. This behavior is reflected in the variation of colors in the shear contours just outside the core region for different test conditions in Figure 36.

Another measure of the shear is the Turbulent Kinetic Energy (TKE). The strong shear gradient across the core/fan jet interface establishes an unstable flow condition, which breaks down into highly turbulent mixing. Consequently, regions of high shear correspond to regions of high TKE. Similarly, test conditions with strong shear velocities would be expected to exhibit strong TKE levels in the mixing layer. This behavior is reflected in the data presented in Figure 38, which illustrates the correlation between TKE levels and shear velocity or velocity gradient for a medium-high shear operating condition (TP9).

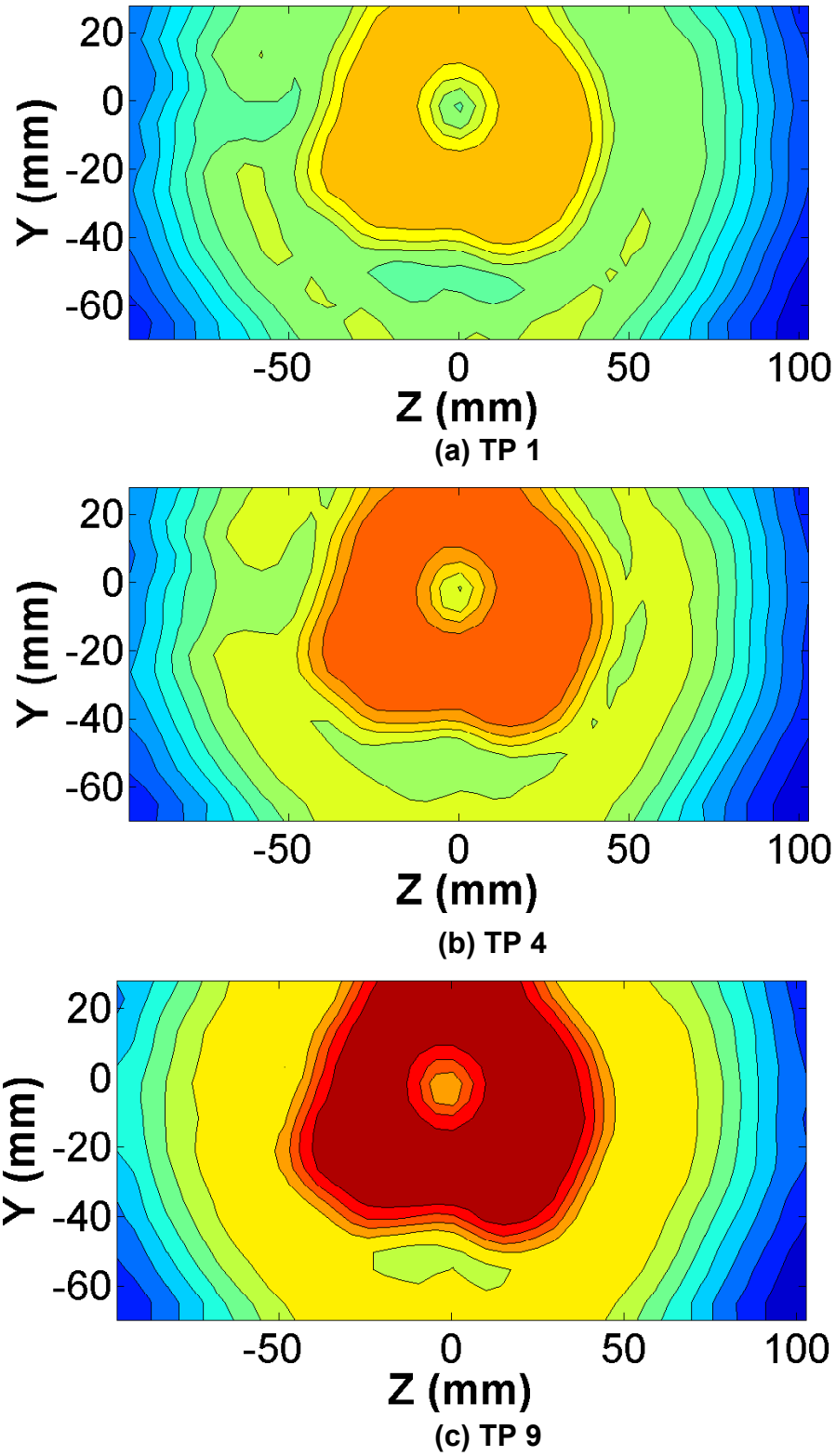

Figure 36. Streamwise velocity contour plots for varying test conditions.

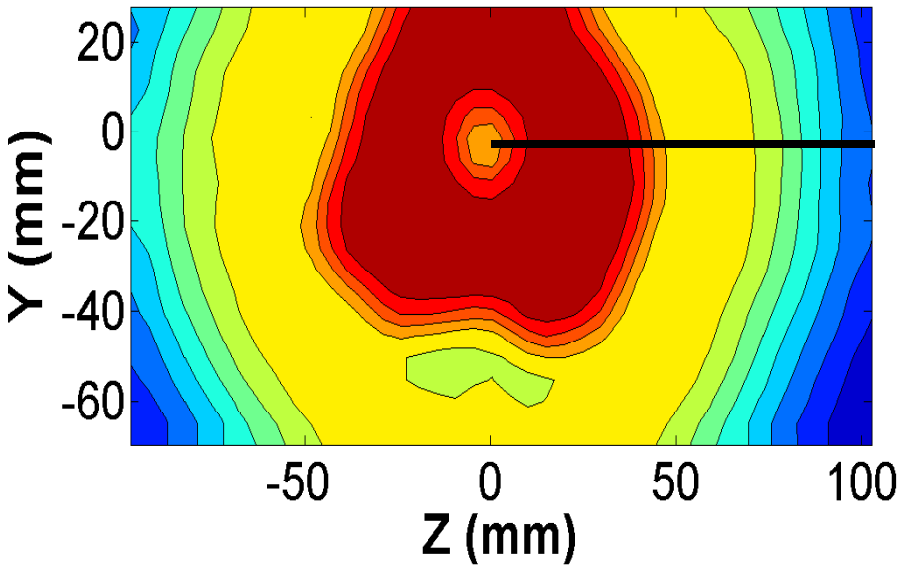

(a) Streamwise Velocity Contour – TP11

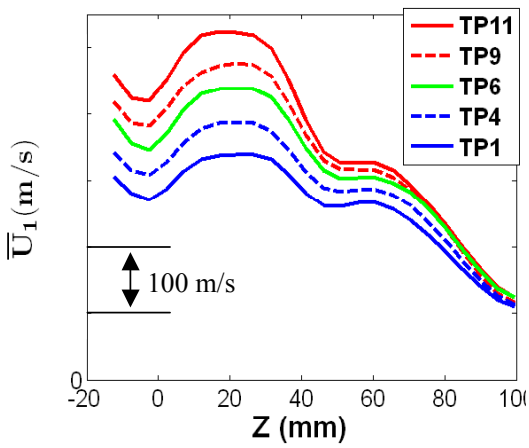

(b) Absolute Scale

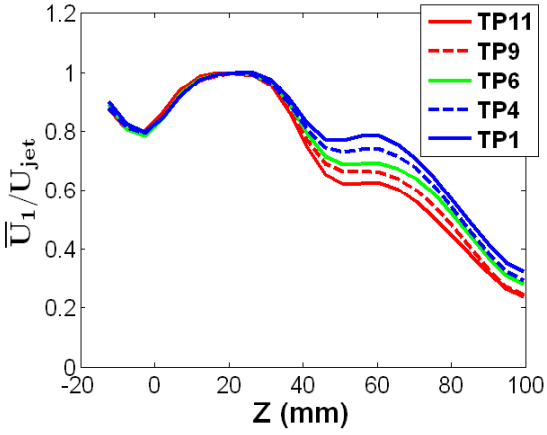

(b) Non-Dimensonal
Relative to Core Velocity

Figure 37. Streamwise velocity comparison for varying test conditions

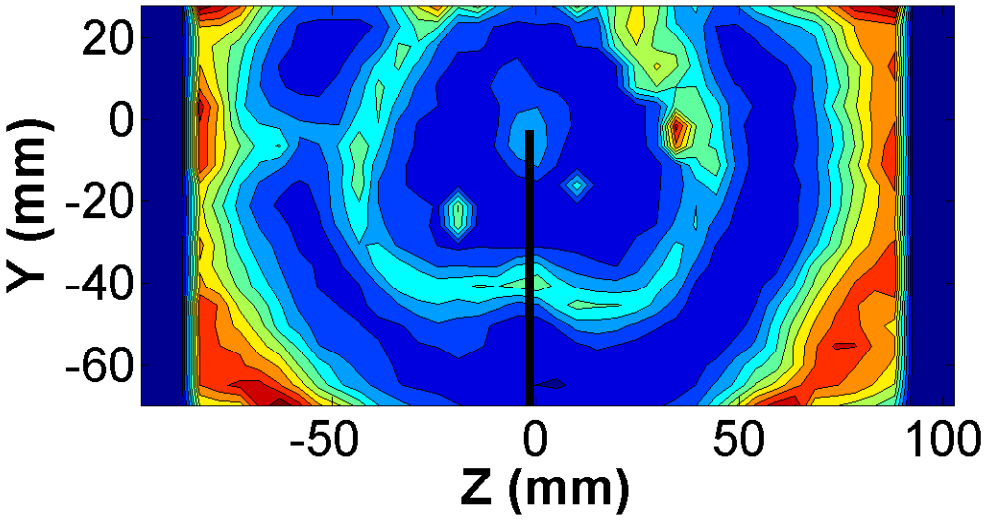

(a) TKE Contour – TP9

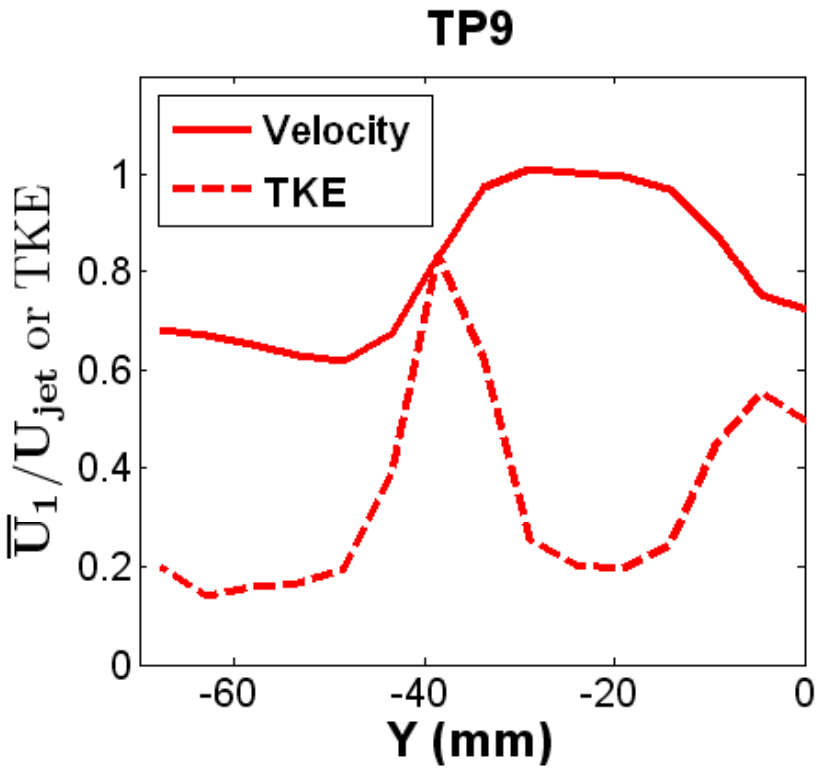

(b) TKE Correlation with Radial Velocity Profile

Figure 38. Turbulent Kinetic Energy Correlation with High Shear Gradient

Impact of Core Chevron Nozzle

The impact of core chevron mixing on the streamwise velocity contours is presented in Figure 39, at two different test points (TP1 & TP9), which correspond to a nominal doubling of the shear velocity. The first features that stand out in the comparison with the baseline conic/conic configuration are the presence of high velocities in the fan stream, and a smaller core peak velocity region. This reflects the cross-stream mixing effects of the streamwise vortices generated by the chevrons. In these comparisons, the fan operating conditions and ambient conditions are the same, so there is very little difference between the fan shear layer in the chevron and baseline cases. Since both configurations used the same fan exhaust nozzle, the differences are confined to the core stream, core/fan shear layer, and the fan stream.

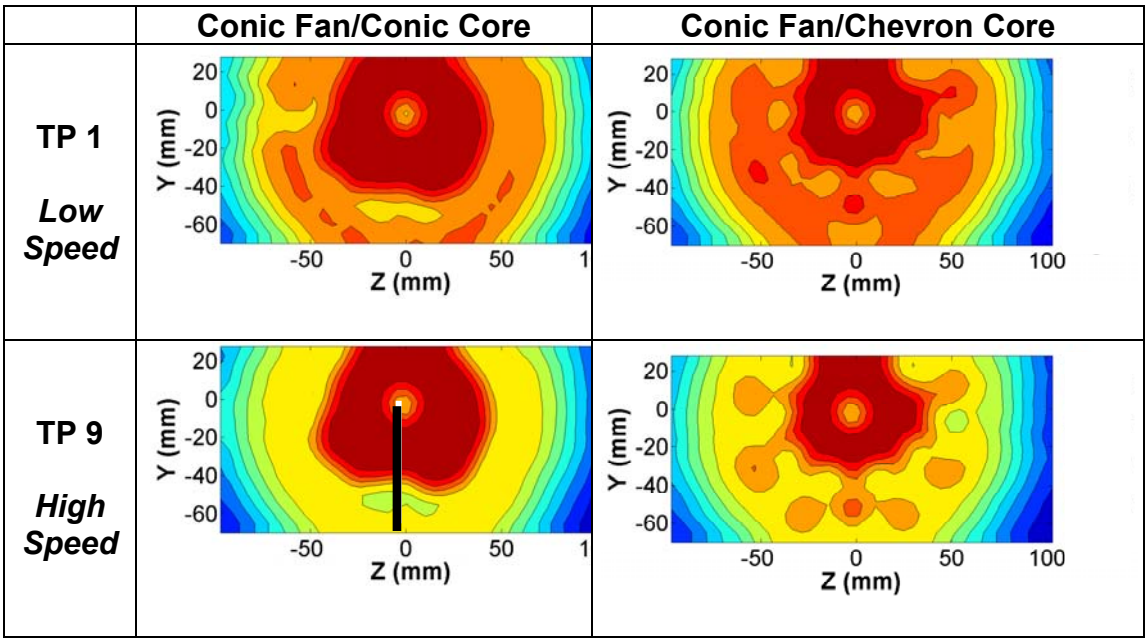

Figure 39. Impact of Core Chevrons on Streamwise Velocity Contours *At Low and High Speed Cycle Conditions*

Corresponding TKE contour comparisons are presented in Figure 40. It was shown in Figure 38 that the TKE correlates with shear velocity, so that regions of high shear would be expected to exhibit high TKE levels. The contour plots capture the azimuthal variations due to the chevrons. Particularly in the TP9 data comparisons, TKE “hot spots” are evident that clearly correspond to similar azimuthal variations in the shear gradient as shown in Figure 39. In addition, the elevated TKE levels in the fan stream reflect the larger scale mixing that occurs as a result of the chevron, relative to the baseline case.

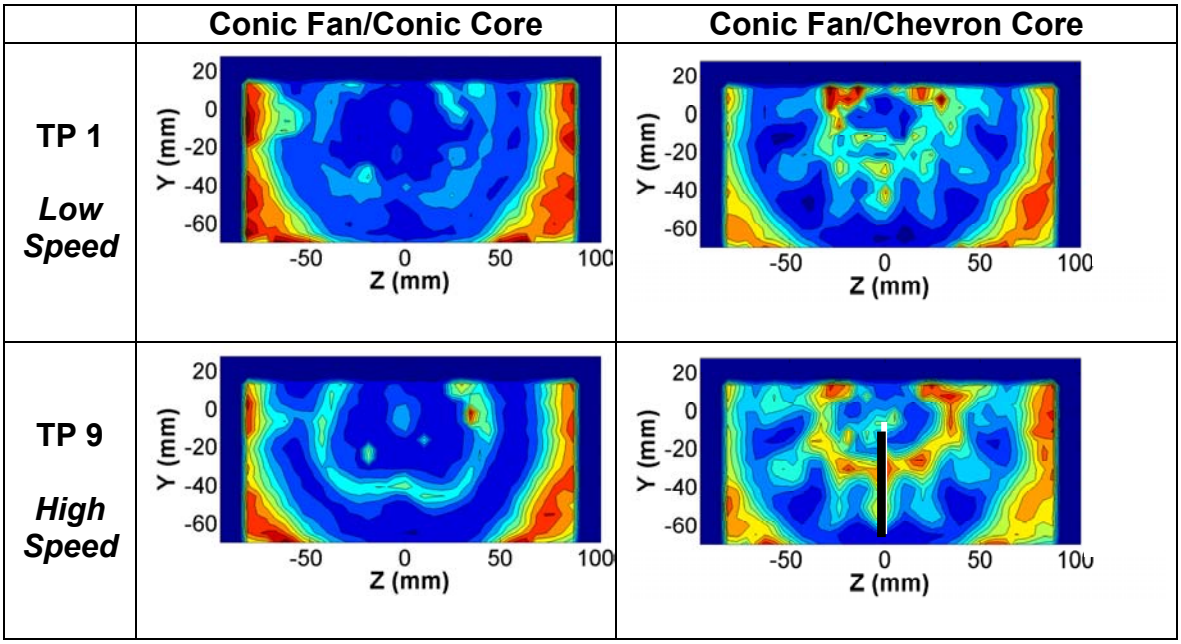

Figure 40. Impact of Core Chevrons on TKE Contours
At Low and High Speed Cycle Conditions

Corresponding radial distribution comparisons of the mean streamwise velocity and TKE, with for the conic fan/conic core and conic fan/chevron core configurations, are shown in Figures 41 and 42. These distributions were taken along the radial cut lines that are illustrated on the baseline and chevron configurations in Figures 39 and 40, respectively. The streamwise velocity comparisons in Figure 41 show the classic chevron behavior. For the baseline configuration, the jet potential core exhibits a large, essentially flat radial region where the peak velocity matches the ideal core velocity. To the right of the core is a reduced velocity region capturing the velocity defect behind the core plug. The baseline gradient is large and steep, and the fan flow velocity is substantially below core levels. For the chevron cases, the velocity defect behind the core plug is essentially unchanged. The rest of the radial distribution exhibits twin peaks, a smaller jet potential core region at the same ideal core velocity, and an outer peak (around Y = -40 mm), which captures the core flow that was ejected into the fan stream, substantially weakening the shear gradient, which is an acoustic source. The corresponding TKE data in Figure 42 reflects the enhanced turbulence levels due to the chevron induced mixing. However, care must be taken when drawing conclusions regarding relative TKE comparisons between the two different test points, since the data presented were extracted from a limited number of images (200), which may be insufficient to fully capture higher order turbulent flow statistics such as TKE.

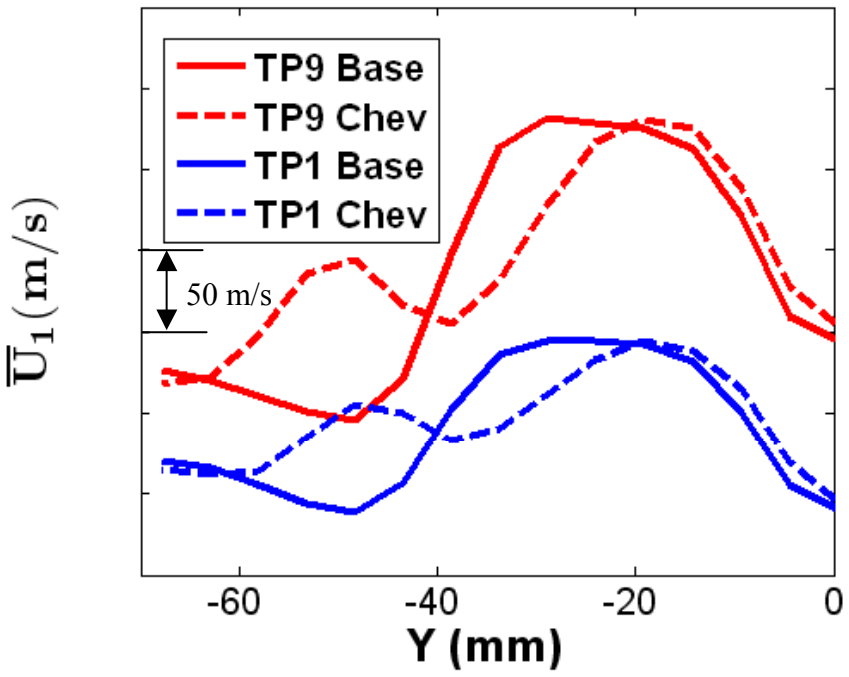

Figure 41. Impact of Core Chevrons on Radial Distribution of Streamwise Velocity

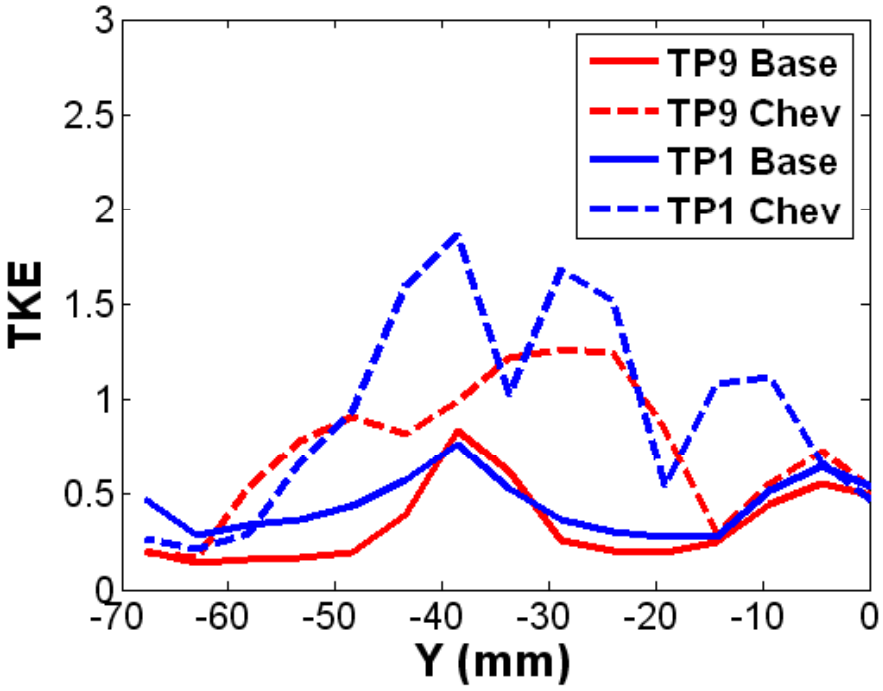

Figure 42. Impact of Core Chevrons on Radial Distribution of TKE

Impact of Fan Exhaust Nozzle Technologies

Given the successful implementation of PIV on the core stream, the camera field of view was re-focused to try and capture the fan/ambient shear layer, to assess the relative mixing of the chevron and new enhanced mixing technology nozzles. For this test configuration, the UC personnel added another supplementary additional seeding source, external to the nozzle, to try to capture the external flow entrained by the fan jet at the static fan/ambient interface. Only limited success was achieved seeding the entrained flow, so the resulting velocity data were restricted by the resulting seed density distributions. Nonetheless, sufficient trends were captured to make relative qualitative comparisons between configurations. Streamwise mean velocity contours for these cases are presented in Figure 43, along with corresponding TKE contours in Figure 44.

Mean streamwise velocity contour comparisons are shown in Figure 43, for the baseline (conic fan/conic core), fan chevron (chevron fan/conic core) and enhanced mixing technology configurations (new devices on fan/conic core), at the same high and low velocity cycle points selected for the core PIV measurement data presented above. Qualitatively, these data demonstrate enhanced mixing of the fan shear layer, relative to the baseline.

	Conic Fan – Conic Core	**Chevron Fan – Conic Core**	**Enhanced Mixing Technology Fan – Conic Core**
TP 1 ***Low Speed***	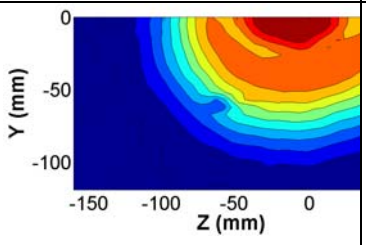	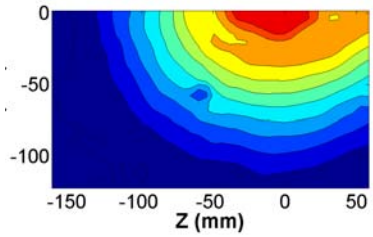	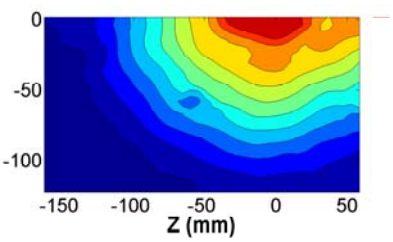
TP 9 ***High Speed***	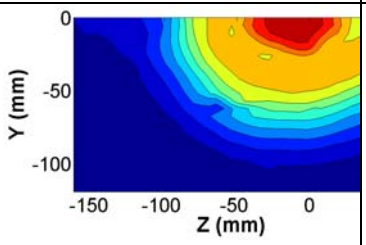	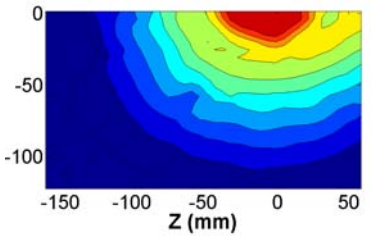	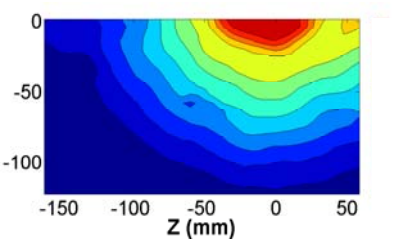

Figure 43. Comparison of Mean Streamwise Velocity Profiles for Baseline, Fan Chevron and Enhanced Mixing Technology Configurations *At Low and High Speed Cycle Conditions*

Corresponding TKE contours are shown in Figure 44. The most striking feature in these plots is a "blacked out" region around Z = -50 mm, Y = -50 mm. In this region, the velocity data are essentially "washed out" by excessive reflection from the core plug tip, making illumination. Consequently, this feature, which was caused by a fundamental limitation in the velocity measurement system, has no physical significance to the measured flow velocities. However, away from the plug, there appeared to be sufficient seed density to support some qualitative comparisons. Comparisons between the Chevron and Baseline configurations suggest that the fan/ambient shear layer had been substantially weakened by the chevron-induced mixing, so that most of the TKE "hot spots" had already mixed out. Similar reductions were achieved for the enhanced mixing technology configuration, except for the extreme right hand side of the contour. It is not clear whether the results in this region (Y = -50 mm, Z = +50 mm) are physical, or another artifact of the seeding and measurement limitations. It should be noted that the velocity measurement plane is approximately 2 fan diameters downstream of the fan exit, as compared to being within a single core diameter of the core stream. This explains the reduction of TKE for the low noise nozzles in the measurement plane, relative to the baseline, as compared to an increase for the core chevron comparison presented above.

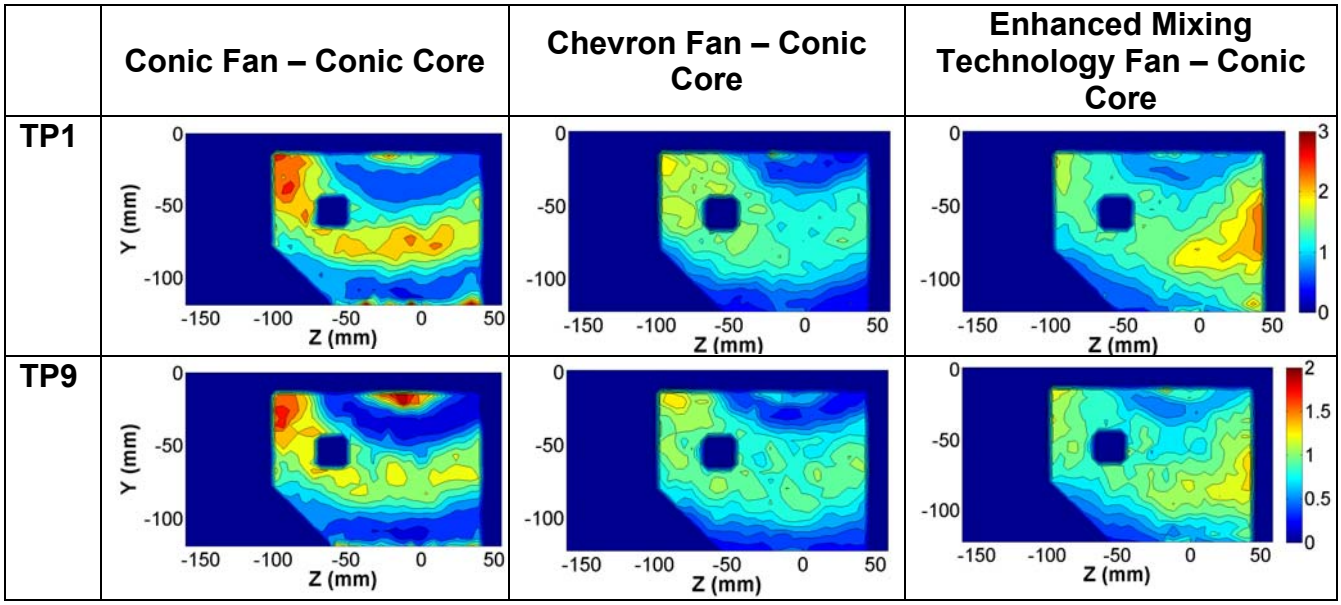

Figure 44. Comparison of TKE Profiles for Baseline, Fan Chevron and Fan Enhanced Mixing Configurations
At Low and High Speed Cycle Conditions

Radial distribution comparisons are presented in Figures 50 and 51, extracted from the corresponding contour data at Z = 0 mm. These data more clearly illustrate the enhanced mixing of each configuration, relative to the baseline. Furthermore, the

reduced TKE levels for the enhanced mixing configuration implies that these devices may be more effective than this particular chevron nozzle, a conclusion that agrees with the acoustic results for each (Configuration 2120.64 vs Configuration 1141.00).

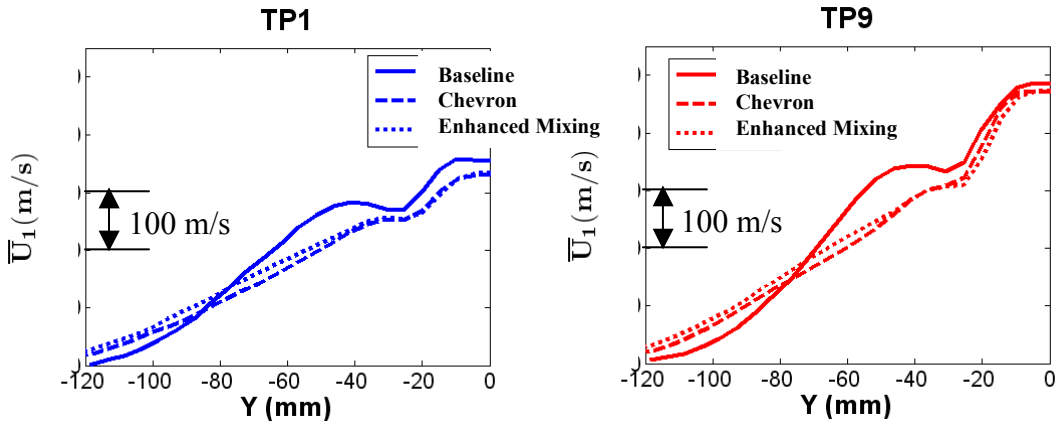

(a) Low-Speed (b) High-Speed

Figure 45. Impact of Fan Exhaust Nozzle Technologies on Radial Distribution of Mean Streamwise Velocity
At Low and High Speed Cycle Conditions

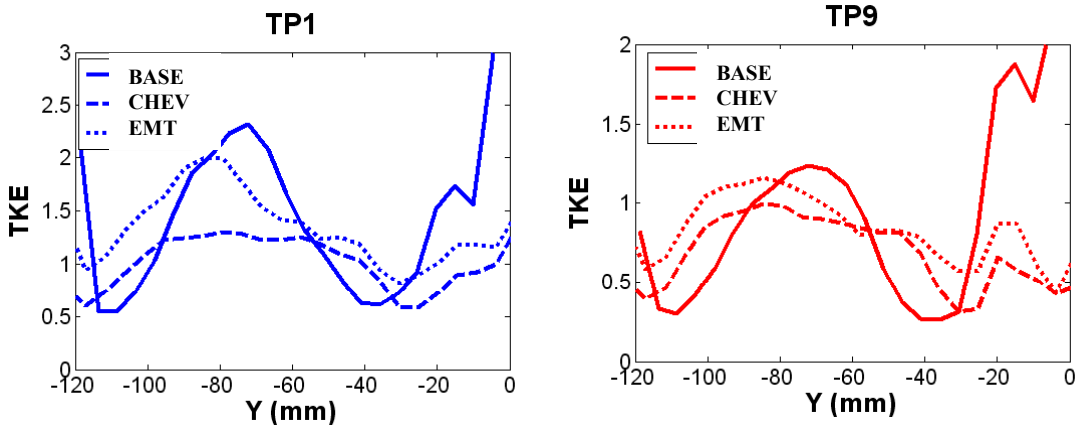

(a) Low-Speed (b) High-Speed

Figure 461. Impact of Fan Exhaust Nozzle Technologies on TKE Radial Distribution
At Low and High Speed Cycle Conditions

Summary of PIV measurements

Overall, Stereo PIV was successfully demonstrated in Cell 41. The data has proven valuable to generate physical insight into the behavior of the baseline configuration at different operating conditions, and illustrate the physical mechanisms governing passively controlled jets.

In general, the PIV confirmed the expected mean velocities in the core and fan streams, and provided general conclusions about the mixing based on the shear velocity gradient and TKE. It was demonstrated that control with chevrons on the core stream enhanced the mixing between the core and fan streams. This behavior corresponds to analytical models, and has been previously demonstrated by other investigators.

Additional comparisons were made between the velocity distribution in the baseline configuration and corresponding data with passive control on the fan stream. The passive control included both a traditional uniform chevron and a new enhanced mixing technology nozzle design. They both had many similarities, but it appeared that the latter configuration spread the jet slightly better and reduced the velocity gradient within the shear layer between the fan stream and ambient stream. This conclusion agrees with the relative acoustic benefit obtained from each test configuration.

Summary – Subtask 3.3.3

An extensive study of new fan exhaust nozzle technologies was performed. Three new uniform chevron nozzles were designed, based on extensive CFD analysis. Two new azimuthally varying variants were defined. All five were tested, along with two existing nozzles, on a representative model-scale, medium BPR exhaust nozzle. Substantial acoustic benefits were obtained from the uniform chevron nozzle designs, the best benefit being provided by an existing design. However, one of the azimuthally varying nozzle designs exhibited even better performance than any of the uniform chevron nozzles. In addition to the fan chevron nozzles, a new technology was demonstrated, using devices that enhance mixing when applied to an exhaust nozzle. The acoustic benefits from these devices applied to medium BPR nozzles were similar, and in some cases superior to, those obtained from conventional uniform chevron nozzles. However, none of the low noise technologies provided equivalent acoustic benefits on a model-scale high BPR exhaust nozzle, similar to current large commercial applications. New technologies must be identified to improve the acoustics of state-of-the-art high BPR jet engines.

Subtask 3.3.3 Variable Geometry Nozzle Design

Task Statement

The goal of this subtask is to develop a feasible passive SMA variable geometry nozzle concept and demonstrate a full-scale single actuator. This task will be worked jointly with NASA GRC, who collaborated on the SMA concepts in the previous Propulsion 21 phases.

Results

GE identified two vendors: Continuum Dynamics, Inc. (CDI), of Ewing, NJ; and Spirit Aerosystems, Inc. (a.k.a. Spirit, formerly Boeing, Wichita), who agreed to jointly develop a full-scale bench top demonstration of an SMA-actuated fan chevron design. CDI's support was provided, with the approval of the NASA program manager, under an existing Phase II SBIR for High Temperature SMA that they are currently working for NASA Glenn Research Center. Based on mutual interest, Spirit agreed to support their portion of the effort under internal research and development funding. Based on the vendors' desire for joint participation, the Propulsion 21 UEET contract resources that were initially identified to support the hardware acquisition under this subtask were re-allocated to expand Subtask 3.3.3 to include PIV velocity characterization of the exhaust nozzle exit flows.

The subject matter of this subtask is considered EAR controlled pursuant to 15 CFR Parts 730-774. Consequently, all details of the final demonstrator and actuator design are outlined in a separate export-controlled GE/CDI/Spirit joint proprietary report, which contains proprietary information from each of the participating companies.

Subtask 3.3.4 Medium BPR Azimuthally Varying Fan Chevron Assessment

Task Statement

The goal of this subtask is to assess the aero-acoustic impacts of 3D CFD based design of azimuthally varying fan chevron exhaust nozzles. This task will be worked jointly with NASA Langley, who collaborated with Boeing on the design of an azimuthally varying fan chevron nozzle for the QTD-2 Demonstrator. The NASA effort will be performed as a "no-cost" addendum to the existing NASA-GRC Space Act Agreement. NASA support will include modeling efforts performed by Eagle Aeronautics and AS&M.

Results

Initial discussions were conducted with NASA Langley to establish a collaborative effort. The intent was to use a "zero-cost" addendum to the existing Space Act Agreement with NASA Glenn, as a vehicle to support the planned joint CFD investigation with NASA Langley. A draft SOW was forwarded to NASA Langley for review and approval. However, agreement could not be reached on the responsibilities and the scope of effort provided by each organization. Consequently, this Subtask was canceled, and two parametric azimuthally varying fan chevron nozzle configurations were added to the low BPR model scale acoustic testing that was conducted under Subtask 3.3.2.

REPORT DOCUMENTATION PAGE	Form Approved OMB No. 0704-0188

1. REPORT DATE *(DD-MM-YYYY)*	2. REPORT TYPE	3. DATES COVERED *(From - To)*
01-06-2008	Final Contractor Report	August 2006-July 2007

4. TITLE AND SUBTITLE
Intelligent Engine Systems
Acoustics

5a. CONTRACT NUMBER
NAS3-01135

5b. GRANT NUMBER

5c. PROGRAM ELEMENT NUMBER
3.3

6. AUTHOR(S)
Wojno, John; Martens, Steve; Simpson, Benjamin

5d. PROJECT NUMBER

5e. TASK NUMBER
37

5f. WORK UNIT NUMBER
WBS 984754.02.07.03.11.03

7. PERFORMING ORGANIZATION NAME(S) AND ADDRESS(ES)
General Electric Aircraft Engines
One Neumann Way
Cincinnati, Ohio 45215

8. PERFORMING ORGANIZATION REPORT NUMBER
E-16494

9. SPONSORING/MONITORING AGENCY NAME(S) AND ADDRESS(ES)
National Aeronautics and Space Administration
Washington, DC 20546-0001

10. SPONSORING/MONITORS ACRONYM(S)
NASA

11. SPONSORING/MONITORING REPORT NUMBER
NASA/CR-2008-215235

12. DISTRIBUTION/AVAILABILITY STATEMENT
Unclassified-Unlimited
Subject Category: 07
Available electronically at http://gltrs.grc.nasa.gov
This publication is available from the NASA Center for AeroSpace Information, 301-621-0390

13. SUPPLEMENTARY NOTES
Responsible person, organization code RB, e-mail: Clayton.L.Meyers@nasa.gov, 216-433-3882.

14. ABSTRACT
An extensive study of new fan exhaust nozzle technologies was performed. Three new uniform chevron nozzles were designed, based on extensive CFD analysis. Two new azimuthally varying variants were defined. All five were tested, along with two existing nozzles, on a representative model-scale, medium BPR exhaust nozzle. Substantial acoustic benefits were obtained from the uniform chevron nozzle designs, the best benefit being provided by an existing design. However, one of the azimuthally varying nozzle designs exhibited even better performance than any of the uniform chevron nozzles. In addition to the fan chevron nozzles, a new technology was demonstrated, using devices that enhance mixing when applied to an exhaust nozzle. The acoustic benefits from these devices applied to medium BPR nozzles were similar, and in some cases superior to, those obtained from conventional uniform chevron nozzles. However, none of the low noise technologies provided equivalent acoustic benefits on a model-scale high BPR exhaust nozzle, similar to current large commercial applications. New technologies must be identified to improve the acoustics of state-of-the-art high BPR jet engines.

15. SUBJECT TERMS
Gas turbine engines; Compressors; Fuel systems; Onboard auxiliary power plants for aircraft

16. SECURITY CLASSIFICATION OF:			17. LIMITATION OF ABSTRACT	18. NUMBER OF PAGES	19a. NAME OF RESPONSIBLE PERSON
a. REPORT	b. ABSTRACT	c. THIS PAGE			STI Help Desk (email:help@sti.nasa.gov)
U	U	U	UU	59	19b. TELEPHONE NUMBER *(include area code)* 301-621-0390